UNIVERSIDADE ESTADUAL PAULISTA
"JÚLIO DE MESQUITA FILHO"
Campus de São José dos Campos
Instituto de Ciência e Tecnologia

TABATA DO PRADO SATO

DESENVOLVIMENTO DE BIOMATERIAIS À BASE DE QUITOSANA: matriz de fibras eletrofiadas para regeneração tecidual e de hidrogel coacervado para entrega controlada de fármaco

2019

TABATA DO PRADO SATO

DESENVOLVIMENTO DE BIOMATERIAIS À BASE DE QUITOSANA: matriz de fibras eletrofiadas para regeneração tecidual e de hidrogel coacervado para entrega controlada de fármaco

Tese apresentada ao Instituto de Ciência e Tecnologia, Universidade Estadual Paulista (Unesp), Campus de São José dos Campos, como parte dos requisitos para obtenção do título de DOUTOR, pelo Programa de Pós-Graduação em ODONTOLOGIA RESTAURADORA.

Área: Prótese Dentária. Linha de pesquisa: Desenvolvimento de Biomateriais e Novas Tecnologias em Odontologia.

Orientador: Prof. Ass. Alexandre Luiz Souto borges

Coorientador: Prof. Dr. Artur José Monteiro Valente

São José dos Campos

2019

Instituto de Ciência e Tecnologia [internet]. Normalização de tese e dissertação [acesso em 2019]. Disponível em http://www.ict.unesp.br/biblioteca/normalizacao

Apresentação gráfica e normalização de acordo com as normas estabelecidas pelo Serviço de Normalização de Documentos da Seção Técnica de Referência e Atendimento ao Usuário e Documentação (STRAUD).

Sato, Tabata Do Prado
Desenvolvimento de biomateriais à base de quitosana: matriz de fibras eletrofiadas para regeneração tecidual e de hidrogel coacervado para entrega controlada de fármaco / Tabata Do Prado Sato. - São José dos Campos : [s.n.], 2019.
85 f. : il.

Tese (Doutorado em Odontologia Restauradora) - Pós-Graduação em Odontologia Restauradora - Universidade Estadual Paulista (Unesp), Instituto de Ciência e Tecnologia, São José dos Campos, 2019.
Orientador: Alexandre Luiz Souto Borges
Coorientador: Artur José Monteiro Valente

1. Quitosana. 2. Nanofibras. 3. Hidrogel. 4. DNA. 5. Sistemas de Liberação de Medicamentos. I. Borges, Alexandre Luiz Souto, orient. II. Valente, Artur José Monteiro, coorient. III. Universidade Estadual Paulista (Unesp), Instituto de Ciência e Tecnologia, São José dos Campos. IV. Universidade Estadual Paulista 'Júlio de Mesquita Filho' - Unesp. V. Universidade Estadual Paulista (Unesp). VI. Título.

Ficha catalográfica elaborada pela Biblioteca Prof. Achille Bassi e Seção Técnica de Informática, ICMC/USP
com adaptações - STATI, STRAUD e DTI do ICT/UNESP.
Renata Aparecida Couto Martins CRB-8/8376

BANCA EXAMINADORA

Prof. Ass. Alexandre Luiz Souto borges (Orientador)
Universidade Estadual Paulista (Unesp)
Instituto de Ciência e Tecnologia
Campus de São José dos Campos

Prof. Dr. Bruno Vinícius Manzolli Rodrigues
Universidade Brasil
Campus Itaquera

Profa. Dra. Fernanda Alves Feitosa
Universidade São Lucas
Faculdade de Odontologia

Prof. Dr. Lafayette Nogueira Júnior
Universidade Estadual Paulista (Unesp)
Instituto de Ciência e Tecnologia
Campus de São José dos Campos

Prof. Dr. Eduardo Shigueyuki Uemura
Universidade Estadual Paulista (Unesp)
Instituto de Ciência e Tecnologia
Campus de São José dos Campos

São José dos Campos, 28 de novembro de 2019.

DEDICATÓRIA

À ciência brasileira.

À educação brasileira.

Ao povo brasileiro, que financiou esta pesquisa.

AGRADECIMENTOS

À **CAPES - Coordenação de Aperfeiçoamento de Pessoal de Nível Superior**, pelo financiamento da bolsa disponibilizada no país e para o Doutorado Sanduíche na Universidade de Coimbra (Processo - 88881.189533/2018-01).

À **Universidade de Coimbra** e ao **Professor Artur Valente** que me receberam de braços abertos e que permitiram um desenvolvimento único dessa pesquisa. Aos **colegas e amigos queridos que fiz em Portugal**. À **Joana**, minha querida companheira de terras lusitanas, uma amiga do outro lado do oceano que nunca sairá do meu coração.

Aos **colegas da Pós-graduação do ICT-Unesp**, meu agradecimento pelo tempo de convivência, pelo aprendizado e, especificamente os da especialidade de Prótese, pela companhia das sextas-feiras dos últimos seis anos. À **Cássia e à Marina**, da Endodontia e Dentística, respectivamente, agradeço pelo apoio, pelas risadas e companheirismo.

Ao **Prof Nelson Luiz de Macedo** pelo suporte inicial ao delineamento da primeira parte desta tese e à amizade de anos que sempre foi um presente.

À **Profa Luana** pelo apoio no desenvolvimento das análises biológicas deste e de outros inúmeros trabalhos. E à sua doutoranda **Daphne**, uma indispensável parceira de pesquisa e uma valorosa amiga.

À disciplina de **Saúde Coletiva**, meu agradecimento sincero pela abertura de uma janela tão maravilhosa da nossa profissão. E em especial à **Profa Symone**, por me permitir, sempre com tanto carinho, estar com ela nessa área, proporcionando tanta aprendizagem.

Aos queridos **funcionários do Departamento de Materiais Odontológicos e Prótese**, que se tornaram grandes amigos durante essa caminhada, a minha gratidão eterna por todo o auxílio, apoio, carinho e inesgotável companheirismo. **Juliane, Lilian, Fernandinho e Marco** fizeram do andar da Prótese um lugar mais parecido com um Lar. **Thaís** obrigada pela amizade, paciência e pelo apoio nas análises e inúmeras micrografias que fizemos

juntas. Ao **Marcos Vestali**, que se foi tão cedo, o meu muito obrigada pelo tempo de convivência. Foi curto, mas extremamente valoroso e cheio de música de qualidade.

Aos queridos **professores da Prótese Parcial Removível** obrigada pelas oportunidades em sala de aula, desde a graduação até agora, quando pude ter a honra de lecionar ao lado de vocês. Obrigada **Prof João** pela oportunidade de trabalhar junto de você nesse Odontomeeting, aprendi muito contigo. Obrigada **Prof Eduardo e Maekawa** por todas as conversas, risadas e ensinamentos. Nenhuma quinta-feira seria a mesma sem vocês. Obrigada **Prof Rodrigo**, por tudo que já me ensinou, pelas conversas e conselhos que levarei para sempre. E, finalmente, **Prof Lafayette**, não há palavras para expressar tamanha a gratidão por tanto carinho, atenção e ensinamentos. Obrigada por todo seu tempo desprendido em clínica comigo, e por todas as vezes que me estendeu a mão.

Aos professores da **Prótese Total** obrigada pela oportunidade de exercer a docência ao lado de vocês nesse ano. Com certeza foi um grande privilégio e cheio de muitos ensinamentos. Obrigada **Carolina Martinelli** que acompanha minha trajetória desde a primeira turma do PreVest Unesp e obrigada **Prof Tarcísio e Profa Paula** pela oportunidade de aprender com vocês.

Ao **Prof Estevão** que me iniciou na vida acadêmica após a graduação, meu agradecimento sincero por tudo. Foi com esse incentivo que tudo começou e por isso serei eternamente grata. E a **Caroline Cotes** que me co-orientou nesse período e me ensinou os caminhos de uma pesquisa de qualidade.

Ao **Programa de Pós-graduação em Odontologia Restauradora**. Ao Professor **Marco Antônio Bottino**. Também à **Lilian Anami** que trabalhou arduamente comigo e me ensinou muito nesta área de pesquisa científica. À nossa equipe da Secretaria da Pós-graduação: **Bruno, Carol e Sandra**. Muito obrigada por todo o auxílio, sempre.

Aos **meus alunos de iniciação científica**. Obrigada por despertarem em mim a paixão por aprender e ensinar dentro da Ciência.

Ao **Instituto de Ciência e Tecnologia Unesp**, na pessoa de sua Diretora, a professora **Rebeca Di Nicoló**, eu agradeço por esses 12 anos de acolhimento, ensinamento e trabalho. Foi minha casa, meu segundo lar, por vezes meu refúgio. Foi de onde veio minha formação desde o cursinho pré-vestibular até esse Doutorado. Muito Obrigada. Ao **Prof Cláudio**, vice-diretor, com quem tive a honra de trabalhar em diversos projetos. A todos os **funcionários desta instituição**, agradeço por todos os serviços prestados e pelos anos de convivência.

Ao **PreVest Unesp e aos meus amados alunos** desses dez anos sendo professora de História e Geografia, minha dívida eterna por terem me mostrado o meu caminho. A minha paixão, lecionar. Ensinar e Aprender. Aprender e ensinar. Com amor, sempre. Agradeço pela esperança que nunca me deixaram faltar e pela força que me deram mesmo quando não sabiam disso.

Ao meu querido orientador **Prof Alexandre**, minha eterna gratidão por todo esse tempo. Passamos por muitas situações juntos nesses últimos anos e, desde a graduação, fizemos esse tempo funcionar muito bem. Nossas descobertas, nossas quedas e nossas vitórias serão sempre motivo de muito orgulho para mim. Levo em meu coração a gratidão pela oportunidade de aprender contigo.

À minha melhor amiga, **Patrícia**. Minha irmã de alma, distantes, ou não, estaremos sempre unidas. Obrigada por você e pela Ali não me deixarem me sentir sozinha, quando longe do Brasil. Me deram um lar num natal que jamais esquecerei.

Ao **Hamilton**, minha gratidão, amizade e amor. Sempre esteve ao meu lado. E, por isso, eu serei eternamente grata.

À minha família, meu **pai Ricardo**, minha **mãe Marli** e meu **irmão Christopher**, meu amor eterno e gratidão pela vida.

" Eu sou o senhor de meu destino; Eu sou o capitão de minha alma. ". William Ernest Henley

SUMÁRIO

Sato TP. Desenvolvimento de biomateriais à base de quitosana: matriz de fibras eletrofiadas para regeneração tecidual e de hidrogel coacervado para entrega controlada de fármaco [tese]. São José dos Campos (SP): Universidade Estadual Paulista (Unesp), Instituto de Ciência e Tecnologia; 2019.

RESUMO

Os atuais avanços no desenvolvimento de biomateriais caminham para 2 áreas promissoras: a de regeneração tecidual e a de entrega controlada de fármacos. Assim, o presente estudo objetivou a síntese e caracterização de diferentes matrizes (fibras e hidrogel) à base de quitosana, a fim de se obter materiais biomiméticos para atuação em ambas áreas. Para regeneração, delineou-se a síntese de um arcabouço de fibras de quitosana com e sem cristais de nanohidroxiapatita onde, para isso, foram eletrofiadas soluções de quitosana (Ch) e de quitosana com nanohidroxiapatita (ChHa). Os espécimes de Ch apresentaram maior homogeneidade e maior diâmetro médio de fibras (690 ± 102 nm) que ChHa (358 ± 49 nm). No teste de viabilidade celular e na atividade da fosfatase alcalina não houve diferença estatística entre os grupos experimentais (Ch e ChHa), porém ambos diferiram do grupo controle ($p < 0,001$). Para o âmbito de liberação de fármacos, sintetizou-se, pela técnica de emulsão, dois tipos de hidrogéis: o primeiro, uma mistura da fase aquosa da solução de Ch (1 mL) e da solução de DNA (1 mL) (1:1) e o segundo, mistura da fase aquosa da solução de Ch (1 mL) e solução de Pectina (1 mL) (1:1). Ambas misturas foram realizadas em álcool benzílico (5 mL) com instrumento de dispersão de alto desempenho (31-34000 rpm min^{-1} por 5 min). Após a obtenção dos géis, 20mg de cada grupo foram imersos em uma solução aquosa de Própolis Verde (PV), na concentração de 70 µg/mL por 2 h e a cinética de liberação do PV foi analisada a 25 e 37ºC em água e saliva artificial. Os espécimes obtidos foram liofilizados e depois caracterizados físico-quimicamente. A presença de pectina e de DNA foi comprovada por FTIR. A sorção de PV induziu uma modificação significativa da superfície do gel. Constatou-se uma separação de fases entre a quitosana e o DNA. A eficiência do encapsulamento não mudou significativamente entre 25 e 37ºC. A cinética de liberação na água ou na saliva apresentou um mecanismo de duas etapas. E os resultados biológicos exibiram que esses materiais são aceitáveis no ambiente biológico. Assim, conclui-se que a matriz de fibras de quitosana com nHAp é capaz de promover diferenciação celular e a matriz de hidrogel de quitosana com Pectina ou DNA possui potencial para a liberação controlada de fármacos.

Palavras-chave: Quitosana. Nanofibras. Hidrogel. DNA. Sistemas de Liberação de Medicamentos

Sato TP. Development of chitosan-based biomaterials: electrospun fiber matrix for tissue regeneration and coacervate hydrogel for controlled drug delivery [doctorate thesis]. São José dos Campos (SP): São Paulo State University (Unesp), Institute of Science and Technology; 2019.

ABSTRACT

Current advances in biomaterial development are moving to 2 promising areas: tissue regeneration and controlled drug delivery. Thus, the present study aimed the synthesis and characterization of different matrices (fibers and hydrogel) based on chitosan, in order to obtain biomimetic materials for performance in both areas. For regeneration, the synthesis of a scaffold of chitosan fibers with and without nanohydroxyapatite crystals was delineated, where chitosan (Ch) and chitosan with hydroxyapatite (ChHa) solutions were electrospun. Ch specimens presented higher homogeneity and larger mean fiber diameter (690±102nm) than ChHa (358 ± 49nm). In the cell viability test and alkaline phosphatase activity there was no statistical difference between the experimental groups. (Ch and ChHa), but both differed from the control group ($p < 0,001$). For the drug release scope, two types of hydrogels were synthesized by the emulsion technique: the first, a mixture of the aqueous phase of Ch solution (1 mL) and DNA solution (1 mL) (1:1) and the second, mixture of the aqueous phase of the Ch solution (1mL) and Pectin solution (1 mL) (1:1). Both mixtures were performed in benzyl alcohol (5 mL) with high performance dispersion instrument (31-34000 rpm min^{-1} for 5 min). After obtaining the gels, 20mg from each group were immersed in an aqueous solution of Propolis Green (PV), at a concentration of 70 µg/mL for 2 h and the release kinetics of PV were analyzed at 25 and 37ºC in water and artificial saliva. The obtained specimens were lyophilized and then physically-chemically characterized. The presence of pectin and DNA was confirmed by FTIR. PV sorption induced a significant modification of the gel surface. A phase separation was found between chitosan and DNA. Encapsulation efficiency did not change significantly between 25 and 37ºC. The release kinetics in water or saliva presented a two-step mechanism. And the biological results showed that these materials are acceptable in the biological environment. Thus, it is concluded that the nHAp chitosan fiber matrix is capable of promoting cell differentiation, whereas the chitosan hydrogel matrix with Pectin or DNA are potential biomaterials for controlled drug release.

Keywords: Chitosan. Nanofibers. Hydrogel. DNA. Drug Delivery Systems.

1 INTRODUÇÃO

A Engenharia de Tecidos (ET) oferece perspectivas promissoras para as áreas de medicina e odontologia atuais, pois visa regenerar tecidos danificados, com materiais biomiméticos que restauram ou conservam a função do tecido vivo (Atala, 2004; Bonassar, Vacanti, 1998).

Através das técnicas de nanofabricação, a ET desenvolve ambientes favoráveis para o desenvolvimento celular, arcabouços com propícias características de adesão de proliferação (Kingsley et al., 2013; Zhang et al., 2018). Já a liberação controlada de fármacos surge no contexto de interações de tecidos com fluidos extracelulares e células especializadas (Chung et al., 2007).

Nanoestruturas poliméricas apresentam características interessantes que suportam uma ampla gama de novas aplicações biotecnológicas (Sandreschi et al., 2016). Neste contexto, uma atenção crescente tem sido dada aos polímeros naturais (Ngwuluka et al., 2016; Titorencu et al., 2017), como os polissacarídeos, devido à sua abundância na natureza e a um apelo global por processos sustentáveis (Honarkar, Barikani, 2009).

Na odontologia, a utilização de nanomateriais já é uma realidade do cenário clínico, como ocorre com dispositivos para diagnóstico de câncer bucal e sistemas de administração de fármacos para interromper a formação de biofilme (AlKahtani, 2018).

Vários são os métodos para fabricação desses materiais, como o *drawing*, uma extrusão por meio de uma secagem giratória (Ondarçuhu, Joachim, 1998; Xing et al., 2008), a síntese *template*, que utiliza uma membrana nanoporosa como um molde de fibras (Feng et al., 2002; Martin, 1996) e a automontagem *(self-assembly)*, uma construção molécula por molécula de estruturas bem definidas (Hiraoka, 2015; Sun et al., 2015). Entretanto, a técnica de eletrofiação

parece ser uma técnica relativamente mais simples e efetiva para a produção de fibras com uma variedade de polímeros de morfologia controlável (Frenot, Chronakis, 2003; Reneker, Chun, 1996; Shanmuga Sundar, Sangeetha, 2012).

Nesse contexto, fibras poliméricas eletrofiadas apresentam propriedades interessantes para muitas aplicações biomédicas, tais como elevada área superficial de contato quando comparadas com outros materiais utilizados nesta área (Huang et al., 2003; Kumar et al., 2016; Mehrasa et al., 2015; Wu et al., 2015).

O processo de eletrofiação é composto por um campo elétrico criado por uma alta tensão aplicada a uma seringa com solução polimérica ou polímero fundido, um capilar metálico e um coletor. Quando a solução é bombeada através de uma bomba de infusão, ou por força gravitacional, atravessa a seringa acoplada ao capilar (eletrodo positivo) e quando o campo elétrico excede a tensão superficial da solução, jatos poliméricos são ejetados em direção ao coletor (eletrodo negativo), posteriormente gerando fibras sólidas devido à evaporação do solvente (Ahmed et al., 2015; Lyons et al., 2004).

Atualmente, biopolímeros naturais são amplamente utilizados em diversas áreas e com várias aplicações alavancadas por métodos como o da eletrofiação (Sell et al., 2010; Soares et al., 2018). Assim, a quitosana, um biopolímero obtido pela desacetilação da quitina, que está presente nos exoesqueletos de crustáceos, insetos, moluscos e parede celular de fungos (Gopalan Nair, Dufresne, 2003; Ifuku, 2014) apresenta, nos últimos tempos, fibras efetivamente eletrofiadas a partir de soluções em ácido acético (Geng et al., 2005; Homayoni et al., 2009) ou usando ácido trifluoroacético (TFA), que pode ser associado com diclorometano (DCM) (Ohkawa et al., 2004).

Estudos recentes sobre a caracterização estrutural das fibras de quitosana (Karpova et al., 2016) apontaram para uma ampla gama de aplicações, desde estabilidade de insulina oral (Chen et al., 2015), regeneração óssea guiada

(Foster et al., 2015; Ma et al., 2014; Qasim et al., 2017), defeitos ósseos alveolares até mesmo nanocomplexos microbicidas para proteção contra infecções por HIV (Boyapalle et al., 2015).

Além disso, muitos estudos associaram a quitosana a outros componentes, como nanopartículas de prata (Hadipour-Goudarzi et al., 2014; Liu et al., 2015), colágeno (Chen et al., 2007; Chen et al., 2010) e extratos naturais (Charernsriwilaiwat et al., 2013) para eletrofiação fibras com diferentes características, tais como a atividade antibacteriana (Hadipour-Goudarzi et al., 2014; Liu et al., 2015), cicatrização alternativa de feridas (Charernsriwilaiwat et al., 2013) e para ambientes adequados à viabilidade celular (Chen et al., 2007; Chen et al., 2010). A hidroxiapatita, importante componente da fase mineral óssea, é um nanomaterial que pode ser incorporado em fibras de quitosana para atividade de regeneração óssea (Kong et al., 2006). Além disso, sob nanoescala, a nanohidroxiapatita (nHAp) possui alta aplicabilidade desde dentifrícios anti-erosão (Aykut-Yetkiner et al., 2014) até engenharia tecidual (Nga et al., 2014; Zhou, Lee, 2011).

Neste estudo, sob essa escala nanométrica, a nHAp foi obtida (Barbosa et al., 2013) para ser incorporada nas fibras de quitosana devido à sua semelhança com a hidroxiapatita do tecido ósseo, reduzindo as limitações biomiméticas.

Além das estruturas fibrilares poliméricas, o presente estudo contemplou a síntese e caracterização de um novo composto de sob uma matriz de hidrogel. Os hidrogéis são conhecidos como redes 3D poliméricas reticuladas, capazes de absorver e reter grandes quantidades de água ou fluidos biológicos (Ma et al., 2016; Peppas, 1986), possuindo uma microestrutura semelhante à matriz extracelular (MEC) (Ma et al., 2016) e significativa biocompatibilidade (Gong, 2006).

Sendo assim, aproveitando a carga positiva do polímero central estudado, a quitosana, decidiu-se investigar a formação de hidrogéis de quitosana-DNA e quitosana-pectina coacervados.

O ácido desoxirribonucleico (DNA) é um biopolímero composto de açúcar desoxirribose, capaz de transportar informações genéticas (Uzumcu et al., 2016). Os hidrogéis de DNA têm propriedades únicas, como biocompatibilidade, ligação seletiva e reconhecimento molecular (Ishizuka et al., 2006; Murakami, Maeda, 2005), criando uma gama de aplicações na liberação controlada de fármacos (Costa et al., 2019; Costa et al., 2011) e engenharia de tecidos (Costa et al., 2014; Li et al., 2013; Um et al., 2006). De fato, entre os polieletrólitos biológicos, o DNA sempre atraiu interesse particular, e existem numerosos estudos sobre as interações entre o DNA e os polications (Costa et al., 2015; Costa et al., 2018; Jorge et al., 2010; Jorge et al., 2013). A formação de hidrogéis coacervados é alcançável quando o DNA é completamente ionizado em pH neutro (Bravo-Anaya et al., 2016a) permitindo a interação com moléculas carregadas positivamente, como a quitosana (Bravo-Anaya et al., 2016b).

Por outro lado, a pectina (P) um polissacarídeo, originário da parede celular de plantas, é usado como polímero gelificante e estabilizante em alimentos e produtos biomédicos devido à influência na saúde humana, como níveis de colesterol e sangramento local (Mohnen, 2008; Thakur et al., 1997), além disso, também é capaz de formar hidrogéis coacervados com quitosana (Cesar Filho et al., 2018; Neufeld, Bianco-Peled, 2017).

Essas duas matrizes de hidrogel (CS-DNA e CS-Pec) foram analisadas no presente estudo na liberação controlada de Própolis Verde (GP), um fitoterápico produzido pelas abelhas *Apis mellifera*, de *Baccharis dracunculifolia* DC (Asteraceae), usado como medicamento anti-inflamatório (de Barros et al., 2007), antifúngico (Santos et al., 2005) e antioxidante (Guimarães et al., 2012;

Nakajima et al., 2007) devido aos seus altos níveis de ácidos fenólicos (Bankova et al., 2000).

Sendo assim, propôs-se neste estudo, a síntese e caracterização de diferentes matrizes (fibras eletrofiadas e hidrogel) à base de quitosana, a fim de se obter biomateriais clinicamente complementares na regeneração tecidual e liberação controlada de fármacos.

2 ARTIGOS

2.1 Artigo – Sato TP, Rodrigues BVM, Mello DCR, Machado JPB, Bottino MC, Vasconcellos LMR, Lobo AO, Borges ALS. Potencial de carregamento de nanohidroxiapatita em fibras de quitosana eletrofiadas: estudos biológicos e morfológicos / *Potential of nanohydroxyapatite loading on electrospun chitosan fibers: biological and morphological studies**

RESUMO

A eletrofiação é uma técnica para produzir fibras poliméricas ultrafinas. A quitosana é um biopolímero usado para esse fim, que origina um biomaterial com atividade antimicrobiana. A hidroxiapatita pode ser associada a este material e, assim, foram produzidas soluções de quitosana a 7 % em peso (Ch) e quitosana / nanohidroxiapatita a 0,5 % em peso (nHAp), ambas usando ácido trifluoroacético e diclorometano como solventes. Todos os materiais eletrofiados foram caracterizados por Microscopia Eletrônica de Varredura, Perfilometria e Microscopia de Força Atômica. As propriedades físico-químicas foram avaliadas por espectroscopia no infravermelho por transformada de Fourier e análises termogravimétricas. Esses materiais também foram investigados usando experimentos celulares *in vitro*. As amostras de Ch apresentaram maior homogeneidade e maior diâmetro médio de fibras (690 ± 102nm) que ChHa (358 ± 49nm). No teste de viabilidade celular e na atividade da fosfatase alcalina não houve diferença estatística entre Ch e ChHa ($p > 0,001$), apenas encontrada entre grupos experimentais e grupos de controle celular ($p < 0,001$), o que confirma que os arcabouços não apresentaram efeitos citotóxicos, mas provam diferenciação celular. Assim, pode-se concluir que o nHAp influenciou nas propriedades topográficas e biológicas, mas não alterou significativamente as propriedades físico-químicas das fibras de quitosana. Curiosamente, todos os arcabouços eletrofiados indicam um bom ambiente para proliferação e diferenciação celular, o que pode abrir uma ampla gama de aplicações desses materiais, como na engenharia de tecidos.

Palavras-chave: Quitosana. Hidroxiapatita. Viabilidade celular.

---

*Artigo elaborado de acordo com as normas do Periódico *Australian Dental Journal* (*Print version* ISSN 1834-7819). Submetido em: 16/04/2018.

ABSTRACT

Electrospinning is a technique to produce ultrathin polymeric fibers. Chitosan is a biopolymer used for this purpose, which originates a biomaterial with antimicrobial activity. Hydroxyapatite can be associate to this material and thus, chitosan 7 wt% (Ch) and chitosan/nanohydroxyapatite 0.5 wt% (nHAp) solutions were produced, both using trifluoroacetic acid and dichloromethane as solvents. All electrospun materials were characterized by Scanning Electronic Microscopy, Profilometry and Atomic Force Microscopy. The physico-chemical properties were assessed by Fourier Transform Infrared Spectroscopy and Thermogravimetry analyses. These materials were also investigated using in vitro cell experiments. The Ch samples showed greater homogeneity and a higher mean diameter (690 ± 102nm) than ChHa (358±49nm). In the cell viability test and alkaline phosphatase activity, there was no statistical difference between Ch and ChHa ($p > 0.001$), only founded between experimental groups and cell control groups ($p < 0.001$) which confirms that scaffolds did not present cytotoxicity effects but prove cellular differentiation. Thus, it can be concluded that the nHAp influenced on the topographical and biological properties but did not changed significantly the physicochemical chitosan fibers properties. Interestingly, all electrospun scaffolds indicate a good environment for cell proliferation and differentiation, which can open a wide range of these materials applications as for tissue engineering.

Keywords: Chitosan. Hydroxyapatite. Cell Survival

1. Introduction

Polymeric nanostructures present interesting features that support a wide range of new biotechnological applications [1]. In this context, growing attention has been given to natural polymers [2, 3], such as polysaccharides, due to their abundance in nature and to a global appeal for sustainable processes [4].

There are several different methods for preparing polymeric fibers, known as drawing [5, 6], template synthesis [7, 8], phase separation [9] and self-assembly [10, 11]. However, electrospinning technique appears to be cost-

effective, reliable and relatively simple technique, which is useful for producing fibers with a polymers variety of controllable morphology [12-14].

Several polymer investigations have been dealing with nano and ultrathin electrospun fibers. Their modifications have led to enforcements expansion [15]. The electrospun fibers present interesting properties for many biomedical applications, such as a high specific surface area and flexibility compared to other materials used in this area [16-19].

Electrospinning consists basically in a high voltage applied into a system constituted by a syringe with polymer solution or melt solution, a metal capillary and a collector. The solution is pumped through an infusion pump, or by gravitational force, through the syringe coupled to capillary (positive electrode). When the electric field exceeds the surface tension, the polymer jets ejected towards the metallic collector (negative electrode), which generates fibers due to the solvent evaporation [20, 21].

Therefore, chitosan, a biopolymer, with interesting properties and the second most abundant biological polysaccharide in the world [22] is obtained by chitin deacetylation, which is present in the crustaceans exoskeletons, insects, mollusks and fungal cell wall [23, 24].

Currently, fibers have been successfully generated by electrospinning of chitosan solutions in 90 wt.% aqueous acetic acid [25, 26] or using trifluoroacetic acid (TFA), that can be associated with dichloromethane (DCM) [27] .

Recent studies have indicated the importance of structural–dynamic characterization of ultrathin chitosan fibers [28] and pointed out their wide range of applications, as oral insulin stability [29], guided bone regeneration [30-32], grafts for alveolar bone defects and microbicides nanocomplexes for protection against HIV infections [33].

In addition to this, many studies have associated chitosan with other components such as silver nanoparticles [34, 35], collagen [36, 37] and natural extracts [38] to electrospun fibers with a wide variety of properties, such as antibacterial activity [34, 35], alternative wound healing [38] and for suitable cell proliferation environments [36, 37].

In this context, hydroxyapatite, an important component of bone mineral phase, is a nanomaterial that can be incorporated in chitosan fibers for bone regeneration activity [39]. Furthermore, at the nanoscale, nanohydroxyapatite (nHAp) form has high applicability from anti-erosion dentifrices [40] until tissue engineering [41, 42].

This particle-size was produced, in this study, to be incorporate in chitosan fibers because of their similarity to bone tissue hydroxyapatite by reducing biomimetic limitations.

Accordingly, the current study proposed to synthesize and characterize electrospun chitosan/nHAp fibers, in order to evaluate the nHAp morphological, physicochemical and biological influences, under specific electrospinning parameters combinations.

2. Methods

2.1 Materials and Experimental procedure

In this study, nHAp crystals were prepared via aqueous precipitation method [43]. Briefly, the nHAp partilces were pruduced using: 10 0mL of 0.167Mof $Ca(NO_3)_2$. $4H_20$ and 100mL of 0.1M of $(NH_4)H_2PO_4$. NH_4OH was added in order to keep the pH~10. The precipitate was subjected to ultrasonic irradiation for 30 min (Ultrasonic Processor 500 W;20 kHz; 13 mm probe; model: SO-VCX-500, SONICS). The resulting suspensions were left to age for

120h. Subsequently, they were filtered, washed with water and dried at 60°C for 4h.This procedure is aimed when a Ca/P of 167 is desired [44].

A typical chitosan solution 7 % (w/v) was prepared by dissolving 0.7 g of medium molecular weight chitosan (75-85 % deacetylated, Sigma-Aldrich, Saint Louis, USA)in 7 mL of Trifluoroacetic acid (TFA) (99% purity, Sigma-Aldrich, Saint Louis, USA) and 3 mL of Dichloromethane (DCM) (98% purity, Sigma-Aldrich, Saint Louis, USA), under constant stirring.

For the chitosan/nHAp solutions, were dissolved 0.7 g of chitosan in 7 mL of TFA, under constant stirring at 30°C. Next, 0.05 g of nHAp were dispersed in 3 mL of DCM and added to the chitosan/TFA solution.

The electrospinning was performed after stirring: solutions were placed in 5 mL plastic syringes (BD, Juiz de Fora, MG, Brazil) couppled to a metallic needle (0.7 mm, INJEX, São Paulo, SP, Brazil) and subjected to the electrospinning process, under different combinations of three parameters: distance (10 to 15cm), voltage (10 to 20kV) and flow rate (0.1 to 0.5 mLh^{-1}).

The fibers were collected at room temperature (25°C) and relative humidity of 30 %, in a collector (10x15 cm) covered with aluminum foil.

The membranes were immersed in 5 M Na_2CO_3 aqueous solution for 3h, at room temperature, in order to neutralize the TFA salts [45]. After the immersion, the membranes were washed with distilled water and dried at room temperature for 24h.

2.2 Morphological and topographical characterization

Scanning Electron Microscope (Inspect S 50, FEI Company, Brno, República Tcheca) (under high vacuum, 15-25 kV and spot 5.0) was used to investigate the fiber's morphology. To taken micrographs a thin layer of gold

under low atmospheric pressure (SC7620 'Mini' Sputter Coater/Glow Discharge System, Emitech, East Sussex, UK) were evaporated on the mats.

The mean diameter of the fibers was calculated using ImageJ software (Versão 1.44o, National Public of Health) from SEM micrographs.Therefore, four samples were selected, two Ch and two ChHa, each one originated from a specific combination of synthesis parameters. ***Table 1*** *shows the groups evaluated and individually parameters to collect micrographs.*

The topographic roughness parameters (Ra = arithmetic average) of membranes were measured by an optical profilometer (Wyko NT 1100, Veeco, Plainview, NY, EUA).

For this study,weused anAtomic Force Microscope (AFM) (Veeco Multimode V, Veeco Instruments, Plainview, NY, USA) located at the LAS/INPE,under intermittent contact mode.

2.3 Physico-chemical characterization

FTIR (Spotlight 400, Perkin-Elmer, Waltham, MA, USA), with an accessory of attenuated total reflectance (ATR-FTIR), was performed at the Instituto de Pesquisa e Desenvolvimento (IP&D-Univap), from 4000 to 500cm^{-1}, using 32 scans and a 4 cm^{-1} resolution.

Thermogravimetry was performed on samples (6-8 mg) placed in a platinum pan and heated from 25ºC to 900°C (10ºC min^{-1}), under N_2atmosphere(flow 50 mL^{-1}) (TGA-50TA, Shimadzu).

2.4 Biological tests

All animal procedures are performed in accordance with the ethics committee guidelines of Sao Jose dos Campos Institute of Science and

Technology, School of Dentistry – UNESP (006/2016-CEUA-ICT-UNESP).And it were realized in accordance with the Ethical Principles for Animal Experimentation, adopted by the Colégio Brasileiro de Experimentação Animal (CONCEA).

After obtained from femurs young adult male Wistar rats, Mesenchymal Stem Cells (MSCs) were cultured in α-MEM (Gibco, Life Technologies, Grand Island, NY, USA), supplemented with 10 % fetal bovine serum (Gibco), 50 mg/ml gentamicin (Gibco), 5 mg/l ascorbic acid (Gibco) and 2.16 g/l a-glycerophosphate (Sigma). Afterwards, the cells were cultured in 24 microplate wells and incubated at 37 with 5 % CO_2. [46]

As control, cells were grown onto culture plate (TCP), and the other groups assessment were Chitosan samples (Ch) and chitosan/nHAp samples (ChHa), for all in vitro analysis.

After 7 days for cultured, MTT colorimetric assay were performed with incubation in 3-(4,5-dimethylthiazol-2-yl)-2,5-diphenyltetrazolium bromide (M5655 Sigma-Aldrich St Louis MO, USA), then the cells were lysed with a propanol acid solution (2-Propanol Sigma-Aldrich St Louis MO, USA) for colorimetric measurement in a spectrophotometer (570 nm with correction at 650 nm) (EL 808 BioTek Instruments, Winooski, USA), as previously describe [47]. The values were expressed in percentage of viable cells compared to the control group.

The data of alkaline phosphatase activity were obtained in quintuplicate, by the release of thymolphthalein by hydrolysis of the thymolphthalein monophosphate substrate, using a commercially available kit (Labtest Diagnóstica SA — Ref. 40, Lagoa Santa, Minas Gerais, Brazil) following the manufacturer's instructions. The test was performed as previously described by Prado et al. [47]. Absorbance was measured in a spectrophotometer at 590 nm and the alkaline phosphatase activity was normalized by total protein content,

which was determinded by Lowry method [48], and the data were expressed as μmol thymolphthalein/h/mg protein.

3. Results and discussion

3.1 Morphological and topographical characterization

The electrospun fibers presents high applicability in tissue regeneration [45-47] by controlling their morphology, porosity and flexibility, being effective to cell scaffolds [48] and topographic surface can change cytoskeletal arrangement and focal adhesion formation [49].

***Figure 1** shows Scanning Electron Micrographs (SEM) of electrospun fibers. A-Ch shows the typical structure in the electrospun chitosan for 0.3 mL/h, 12 cm, 10 kV and B-Ch for 0.3 mL/h, 15 cm, 10 Kv. C-ChHa shows the electrospun chitosan/nHAp for 0.5 mL/h, 12 cm, 17 kV and D-ChHa for 0.5 mL/h, 15 cm, 17 kV. All Ch samples showed homogeneous fibers' networks, whilstall samples obtained from ChHa presented beads and some discontinuities, as can be seen in.*

Some studies demonstrated that higher voltage offers the greater probability of beads formation [49, 50] and voltage can influence the fiber diameter, but should vary according to the polymer solution and on the distance between the capillary and the collector [51].

In this study, temperature ($25^{O}C \pm 2$) and relative humidity ($40\% \pm 5$) are standardized whereas these elements were extremely important to the electrospinning effectiveness [50-52]. There are reports that relative humidity can modify the fibers diameter [52] and temperature variation can also cause this change, which can be associated with the solvent evaporation rate and solution viscosity [52]. As expected, Ch and ChHa solutions were working

*parameters on electrospinning sensitive and the effective fiber formation was only found under specific combinations (**Table 1**).*

The neutralization procedure was necessary to realize the scaffolds usefulness in areas that require a contact with neutral or weak basic aqueous middle [45] and the enviroment neutralization should be equally considered to obtain optimal water absorption [53].

*The average diameter fiber ranged from 324 nm (D-ChHa) to 763nm (B-Ch). It was also observed sensibility to the nHAp loading, with a significant ChHa diameter decrease. In the **Fig 2** the measured values distribution is presented in histograms.*

The diameter distribution presented significant difference between A-Ch and B-Ch, that could be related with distance decrease, between the capillary and the collector, which culminates in the increase of electric field, responsible for fibers stretching, implying a diameter fiber decrease [54, 55].

During an electrospinning process, it is very important to produce the fibers with minimum possible diameter, due the thinner and homogeneous fibers that provide maximum surface area and porosity, which results in a higher adsorbents efficiency [56] Thus, it is aimed to obtain a biomimetic characterization of the extracellular matrix.

It was observed that fibers formed at lower collector distance (7.5 cm), presented bead formation. It could be due to the higher electrical forces on the jet which made it unstable. Under controlled distance increase (13.75 cm), the solution jet stability was also increased, in order to a homogeneous fibers synthesis and lower diameters. In addition to that, with 20 cm distance, fibers with higher diameter were formed, perhaps, accordingly to the strength of electrical force on the spinning solution decrease [57].

In this sense, is reported in literature that the diameter could be influenced by whether complete crystallization of polymer chains took place before or after the electrospinning jet has reached the collector [58].

The scaffold surface morphology has an important role in tissue engineering [59], and studies have shown the chemistry, geometry and topography importance to cell behavior [60, 61]. ***Figure 3*** *shows the images obtained from A-Ch, B-Ch, C-ChHa and D-ChHa where it is possible to analyze 2D (right) and 3D (left) perspectives.*

This analysis presented more homogeneous Ch than ChHa fibers. There was average Ra (Roughness average) 9.22 μm ± 1.94 for Ch and 2.92 μm ± 0.29 for ChHa, with statistically significant difference between them (p = 0.0052). Thus, the ChHa diameter fiber reduction can be attributed to the fact that electrospun polymer nanofibers, with the lowest fiber diameter, were obtained at the highest electrical conductivity [62] and consequent increase the neat charge density in the jet due to nHAp presence.

*In this context, AFM analysis (****Fig 4****) showed that ammounts of nHAp altered the membranes surface morphology.*

Through the AFM analysis it was possible to observe better homogeneity and smoothness in the Ch fibers compared to the high roughness of ChHa. ***Figure 4.A*** *showed a more homogeneous surface and clear disclosure of ultrathin fibers with about approximately 0.6 μm. In contrast,* ***Fig 4.B*** *showed an irregular and rough surface. It can be explained by the nHAp increased content, that changes scaffolds microstructure, attributed to the gradual weakening of the intermolecular interactions as the hydrogen bonding between the chitosan fiber molecules [63].*

The FTIR spectra of all samples are shown in ***Fig 5.A****.*

*It is possible to identify the characteristic bands of electrospun Ch and ChHa (****Fig 5.B****) at 720, 800 and 840 cm^{-1}. The nHAp analysis shows a band in*

the range of 550 cm^{-1}. Already at 1644 cm^{-1} and 1552cm^{-1} transmitance occurs, as seen in ***Fig 5.C.***

*The FTIR analysis presented characteristic transmittance bands that reveals TFA salt formation (**Fig 5.B**) settling to three bands (720, 800 and 840 cm^{-1}) - that disappeared after alkaline treatment - and amino group (-NH3+) around 1675 and 1540 cm^{-1}[64].*

In fact, the chitosan amino groups are reported as D-glucosamine residues which can be protonated, providing solubility in acid aqueous solutions [65, 66].

Chitosan dissolved in TFA is a very strong acid dissolution that can occurs not only by a protonation of the amino groups but also by esterification, and this esterified product is more soluble than chitosan by itself, and which, by FTIR verified the presence of TFA salts, that can explain the immediate dissolution of ChHa and Ch scaffolds in water presence.

For this reason, it is understood that the TFA choice, as chitosan solvent, must aim the neutralization and residual elimination [45, 67] on the electrospun ultrathin fibers, as an important applicability feature in the cellular proliferation context.

The same amine groups are reported in the salt formation when combined with TFA. It was observed that the TFA destroyed the intermolecular interactions between the chains of chitosan and facilitated the electrospinning process [68]. This is showed in transmittance bands by the FTIR analysis, that according to some studies disappear after alkaline treatment [67].

Regarding to nHAp, OH flexural vibration appeared as a weak peak in the low-frequency band of 550cm^{-1} as some studies [69] found in 669 cm^{-1}, that verifies the presence of amino groups (-NH^{+3}). Simultaneously, 1644 cm^{-1} and 1552cm^{-1} absorbance can be attributed to the two types of variations, H-O-H (water) flexural vibration and carbonyl stretching (C=O), respectively [64, 70].

Studies it was observed that observed OH stretching (3500 cm^{-1} FTIR) when nHAp was subjected to high temperatures (> 800 ° C) [71]. Moreover, at high temperatures (> 600°C), this weight loss may be assigned to decarboxylation of nHAp, releasing CO_2 (g) and causing condensation of HPO_4^{2-} releasing water [71].

Thus, chitosan hydrophilicity is partly influenced by the presence of amine groups, that are vital in the dissolution context of this material in an acid solution and in the resistance of chemical and biological degradation [72].

*According to thermal tests, the results were included at different stages (**Table 2**). The first one correspond to absorbed/adsorbed loss of water, and the second one, was about thermal decomposition, until reaching a maximum degradation, under a maximum decomposition temperature.*

*The electrospun Ch had the first mass loss stage at 25 °C to 118 °C range, with a mass loss of 9.0 %; a second stage in the range 126 °C to 280 °C, with a weight loss of 40.1 %; and a third and final stage, between 280-431 ºC, with a weight loss of 24.0 %. **Figure 6** shows the thermogravimetric analyses of a chitosan sample average molecular weight of powder, chitosan and electrospun chitosan with nHAp.*

ChHa had the first stage between 25 °C and 120 °C, with a weight loss of 10.9 %; the second stage between 125 ºC and 288 ºC, with a weight loss of 40.1 %; and a third and final stage, between 288-435 ºC, with a weight loss of 21.5 %.

Already isolated nHAp features three weight loss stages, in the ranges of 25-120 °C (loss of 4.58%), 120-390 °C (loss of 5.78%) and 390-500 °C (loss of 1.1%), all relating to chemical and physical loss of water. Among 500-1000 °C, the mass nHAp varied very little (loss of 0.11 %).

*For the biological tests, the cell viability was obtained by MTT test, and the results showed in **Fig 7,** measurement of cell viability (viable cells*

comparing to control group), that the biomaterial influenced positively the cell culture. Therefore, there was no statistical difference between Ch and ChHa ($p > 0.001$). The control group exibhited a lower quantify of cell proliferation showing statistsical difference with experimental groups ($p < 0.001$). The results showed that the scaffolds did not present cytotoxicity effects once the cell proliferation it bigger that control group cytotoxicity effects.

The cell-material interaction include adhesion and spreading of osteoblast cell on the material surface, which will influence following processes of cell proliferation and differentiation [73]. Previous studies observed that the material surface properties can regulate these process [74, 75], with roughness being important factor that affects cell adhesion and proliferation [76]. Although the roughness rate between the experimental groups showed a statistical difference, this factor did not influence the cell viability rate. However, a tendency was observed for the viable cell increase in the rougher fibers represented by ChHa.

It is suggested, from the present study, that this value was similar between the experimental groups because the Ch fiber exhibited another factor, that acts on the cellular behavior, a structural arrangement, allowing also favorable cell viability. Then, both fibers constituted the propitious cell metabolism environment.

The rates of cell viability exhibited by both groups make them suitable for biomedical use according to the International Organization for Standardization (ISO) and national standards for Biological Evaluation of Medical Devices, ISO 10993-5 [77].

*Regarding to osteoblastic differentiation, the association of hydroxiapatite with polymers have present positive results into cell metabolism [78]. Statistical difference was presented among the groups ($p < 0.001$), the ChHa group provided higher means of ALP activity (**Fig 8**), spite wihtout*

different with Ch group. Alkaline phosphatase is known to be an early indicator of osteoblast differentiation, and your expression is considered to be a functional parameter in vitro, reflecting the progress of cell differentiation [79].

It is important to note that among all natural polymers, chitosan (CS) was selected for this study due to its unique structural characteristics similar to GAGs in the ECM [76], and it is suggested that its association with nHAp did not provide greater cell differentiation capacity due to the great positive chitosan influence.

The results exhibited represents that these new biomaterials are acceptable in the biological environment, with the osteogenic differentiation possibility, and can provide evidence for the potential of biomimetic ultrathin chitosan fibers in tissue engineering and clinical application [80].

Thus, it was reasonable to conclude that the prepared nanofibrous matrix coated with chitosan and nHAp could be potential candidates for the regeneration of bone, once that the tendency can be observed in higher level of ChHa group cell activity.

4. Conclusions

Thus, it is concluded that the addition of nHAp can influence the topographical and morphological aspects of ultrathin chitosan fibers, in order to reduce the average diameter and to increase surface roughness, which can change its behavior towards by the modification in the development and cell proliferation.

In contrast, nHAp crystals did not influence the physicochemical characteristics of the chitosan scaffolds.

And the fibers biological tests with and without nHAp showed to be a good environment for cell proliferation and differentiation, which open a wide

range of applications of these materials for tissue engineering and clinical potentials.

Acknowledgements

The authors would like to thank Sao Paulo Research Foundation (FAPESP, grants numbers: 2011/17877-7 and 2011/20345-7); National Council for Scientific and Technological Development (CNPq grants numbers 310973/2014-7 and 310659/2014-0), Coordination for the Improvement of Higher Education Personnel (CAPES, grant numbers 88881.120138/2016-01 and 88881.120221/2016-01) and to Universidade Brasil for the scholarships.

References

[1] S. Sandreschi, A.M. Piras, G. Batoni, F. Chiellini, Perspectives on polymeric nanostructures for the therapeutic application of antimicrobial peptides, Nanomedicine, 11 (2016) 1729-1744.

[2] N.C. Ngwuluka, N.A. Ochekpe, O.I. Aruoma, Functions of Bioactive and Intelligent Natural Polymers in the Optimization of Drug Delivery, Industrial Applications for Intelligent Polymers and Coatings, Springer2016, pp. 165-184.

[3] I. Titorencu, M. Georgiana Albu, M. Nemecz, V. V Jinga, Natural Polymer-Cell Bioconstructs for Bone Tissue Engineering, Current stem cell research & therapy, 12 (2017) 165-174.

[4] H. Honarkar, M. Barikani, Applications of biopolymers I: chitosan, Monatshefte für Chemie - Chemical Monthly, 140 (2009) 1403-1420.

[5] C. Joachim, Drawing a single nanofibre over hundreds of microns, EPL (Europhysics Letters), 42 (1998) 215.

[6] X. Xing, Y. Wang, B. Li, Nanofibers drawing and nanodevices assembly in poly (trimethylene terephthalate), Optics express, 16 (2008) 10815-10822.

[7] L. Feng, S. Li, H. Li, J. Zhai, Y. Song, L. Jiang, D. Zhu, Super-Hydrophobic Surface of Aligned Polyacrylonitrile Nanofibers, Angewandte Chemie International Edition, 41 (2002) 1221-1223.

[8] C.R. Martin, Membrane-Based Synthesis of Nanomaterials, Chem. Mater., 8 (1996) 1739-1746.

[9] P.X. Ma, R. Zhang, Synthetic nano-scale fibrous extracellular matrix, J Biomed Mater Res, 46 (1999) 60-72.

[10] S. Hiraoka, What Do We Learn from the Molecular Self-Assembly Process?, Chemical record, DOI 10.1002/tcr.201510005(2015).

[11] Y. Sun, L. Scarabelli, N. Kotov, M. Tebbe, X.M. Lin, W. Brullot, L. Isa, P. Schurtenberger, H. Moehwald, I. Fedin, O. Velev, D. Faivre, C. Sorensen, R. Perzynski, M. Chanana, Z. Li, F. Bresme, P. Kral, E. Firlar, D. Schiffrin, J.B. Souza Junior, A. Fery, E. Shevchenko, O. Tarhan, A.P. Alivisatos, S. Disch, R. Klajn, S. Ghosh, Field-assisted self-assembly process: general discussion, Faraday discussions, 181 (2015) 463-479.

[12] A. Frenot, I.S. Chronakis, Polymer nanofibers assembled by electrospinning, Curr. Opin. Colloid Interface Sci., 8 (2003) 64-75.

[13] S. Shanmuga Sundar, D. Sangeetha, Investigation on sulphonated PEEK beads for drug delivery, bioactivity and tissue engineering applications, J Mater Sci, 47 (2012) 2736-2742.

[14] D.H. Reneker, I. Chun, Nanometre diameter fibres of polymer, produced by electrospinning, Nanotechnology, 7 (1996) 216-223.

[15] A. Greiner, J.H. Wendorff, Electrospinning: a fascinating method for the preparation of ultrathin fibers, Angewandte Chemie International Edition, 46 (2007) 5670-5703.

[16] Z.-M. Huang, Y.-Z. Zhang, M. Kotaki, S. Ramakrishna, A review on polymer nanofibers by electrospinning and their applications in nanocomposites, Composites science and technology, 63 (2003) 2223-2253.

[17] Y. Wu, S. Feng, X. Zan, Y. Lin, Q. Wang, Aligned Electroactive TMV Nanofibers as Enabling Scaffold for Neural Tissue Engineering, Biomacromolecules, DOI 10.1021/acs.biomac.5b00884(2015).

[18] M. Mehrasa, M.A. Asadollahi, K. Ghaedi, H. Salehi, A. Arpanaei, Electrospun aligned PLGA and PLGA/gelatin nanofibers embedded with silica nanoparticles for tissue engineering, International Journal of Biological Macromolecules, 79 (2015) 687-695.

[19] P.S. Kumar, S. Jayaraman, G. Singh, Polymer and Composite Nanofiber: Electrospinning Parameters and Rheology Properties, Rheology and Processing of Polymer Nanocomposites, DOI (2016) 329-354.

[20] F.E. Ahmed, B.S. Lalia, R. Hashaikeh, A review on electrospinning for membrane fabrication: challenges and applications, Desalination, 356 (2015) 15-30.

[21] J. Lyons, C. Li, F. Ko, Melt-electrospinning part I: processing parameters and geometric properties, Polymer, 45 (2004) 7597-7603.

[22] S. Torres-Giner, M.J. Ocio, J.M. Lagaron, Novel antimicrobial ultrathin structures of zein/chitosan blends obtained by electrospinning, Carbohydrate Polymers, 77 (2009) 261-266.

[23] K. Gopalan Nair, A. Dufresne, Crab Shell Chitin Whisker Reinforced Natural Rubber Nanocomposites. 1. Processing and Swelling Behavior, Biomacromolecules, 4 (2003) 657-665.

[24] S. Ifuku, Chitin and Chitosan Nanofibers: Preparation and Chemical Modifications, Molecules, 19 (2014) 18367.

[25] X. Geng, O.-H. Kwon, J. Jang, Electrospinning of chitosan dissolved in concentrated acetic acid solution, Biomaterials, 26 (2005) 5427-5432.

[26] H. Homayoni, S.A.H. Ravandi, M. Valizadeh, Electrospinning of chitosan nanofibers: processing optimization, Carbohydrate polymers, 77 (2009) 656-661.

[27] K. Ohkawa, D. Cha, H. Kim, A. Nishida, H. Yamamoto, Electrospinning of chitosan, Macromolecular Rapid Communications, 25 (2004) 1600-1605.

[28] S. Karpova, A. Ol'khov, A. Iordanskii, S. Lomakin, N. Shilkina, A. Popov, K. Gumargalieva, A. Berlin, Nonwoven blend composites based on poly (3-hydroxybutyrate)–chitosan ultrathin fibers prepared via electrospinning, Polymer Science Series A, 58 (2016) 76-86.

[29] J. Chen, C. Liu, W. Shan, Z. Xiao, H. Guo, Y. Huang, Enhanced stability of oral insulin in targeted peptide ligand trimethyl chitosan nanoparticles against trypsin, J Microencapsul, DOI 10.3109/02652048.2015.1065920(2015) 1-10.

[30] L.J.R. Foster, S. Ho, J. Hook, M. Basuki, H. Marçal, Chitosan as a Biomaterial: Influence of Degree of Deacetylation on Its Physiochemical, Material and Biological Properties, PLoS ONE, 10 (2015) e0135153.

[31] S. Ma, Z. Chen, F. Qiao, Y. Sun, X. Yang, X. Deng, L. Cen, Q. Cai, M. Wu, X. Zhang, P. Gao, Guided bone regeneration with tripolyphosphate cross-linked asymmetric chitosan membrane, Journal of Dentistry, 42 (2014) 1603-1612.

[32] S.B. Qasim, S. Najeeb, R.M. Delaine-Smith, A. Rawlinson, I. Ur Rehman, Potential of electrospun chitosan fibers as a surface layer in functionally graded GTR membrane for periodontal regeneration, Dental Materials, 33 (2017) 71-83.

[33] S. Boyapalle, W. Xu, P. Raulji, S. Mohapatra, S.S. Mohapatra, A Multiple siRNA-Based Anti-HIV/SHIV Microbicide Shows Protection in Both In Vitro and In Vivo Models, PLoS One, 10 (2015) e0135288.

[34] E. Hadipour-Goudarzi, M. Montazer, M. Latifi, A.A.G. Aghaji, Electrospinning of chitosan/sericin/PVA nanofibers incorporated with in situ synthesis of nano silver, Carbohydr. Polym., 113 (2014) 231-239.

[35] Y. Liu, Y. Liu, N. Liao, F. Cui, M. Park, H.-Y. Kim, Fabrication and durable antibacterial properties of electrospun chitosan nanofibers with silver nanoparticles, Int. J. Biol. Macromol., 79 (2015) 638-643.

[36] Z. Chen, X. Mo, F. Qing, Electrospinning of collagen–chitosan complex, Mater. Lett., 61 (2007) 3490-3494.

[37] Z.G. Chen, P.W. Wang, B. Wei, X.M. Mo, F.Z. Cui, Electrospun collagen–chitosan nanofiber: A biomimetic extracellular matrix for endothelial cell and smooth muscle cell, Acta Biomater., 6 (2010) 372-382.

[38] N. Charernsriwilaiwat, T. Rojanarata, T. Ngawhirunpat, M. Sukma, P. Opanasopit, Electrospun chitosan-based nanofiber mats loaded with Garcinia mangostana extracts, Int. J. Pharm., 452 (2013) 333-343.

[39] L. Kong, Y. Gao, G. Lu, Y. Gong, N. Zhao, X. Zhang, A study on the bioactivity of chitosan/nano-hydroxyapatite composite scaffolds for bone tissue engineering, European Polymer Journal, 42 (2006) 3171-3179.

[40] A. Aykut-Yetkiner, T. Attin, A. Wiegand, Prevention of dentine erosion by brushing with anti-erosive toothpastes, J Dent, 42 (2014) 856-861.

[41] N.K. Nga, L.T. Giang, T.Q. Huy, P.H. Viet, C. Migliaresi, Surfactant-assisted size control of hydroxyapatite nanorods for bone tissue engineering, Colloids Surf., B, 116 (2014) 666-673.

[42] H. Zhou, J. Lee, Nanoscale hydroxyapatite particles for bone tissue engineering, Acta Biomater, 7 (2011) 2769-2781.

[43] M.C. Barbosa, N.R. Messmer, T.R. Brazil, F.R. Marciano, A.O. Lobo, The effect of ultrasonic irradiation on the crystallinity of nano-hydroxyapatite produced via the wet chemical method, Mater Sci Eng C Mater Biol Appl, 33 (2013) 2620-2625.

[44] M.C. Barbosa, N.R. Messmer, T.R. Brazil, F.R. Marciano, A.O. Lobo, The effect of ultrasonic irradiation on the crystallinity of nano-hydroxyapatite produced via the wet chemical method, Materials Science and Engineering: C, 33 (2013) 2620-2625.

[45] P. Sangsanoh, P. Supaphol, Stability improvement of electrospun chitosan nanofibrous membranes in neutral or weak basic aqueous solutions, Biomacromolecules, 7 (2006) 2710-2714.

[46] C. Maniatopoulos, J. Sodek, A. Melcher, Bone formation in vitro by stromal cells obtained from bone marrow of young adult rats, Cell and tissue research, 254 (1988) 317-330.

[47] R.F.d. Prado, F.S. de Oliveira, R.D. Nascimento, L.M.R. de Vasconcellos, Y.R. Carvalho, C.A.A. Cairo, Osteoblast response to porous titanium and biomimetic surface: In vitro analysis, Materials Science and Engineering: C, 52 (2015) 194-203.

[48] O.H. Lowry, N.J. Rosebrough, A.L. Farr, R.J. Randall, Protein measurement with the Folin phenol reagent, Journal of biological chemistry, 193 (1951) 265-275.

[49] J. Deitzel, J. Kleinmeyer, D. Harris, N.B. Tan, The effect of processing variables on the morphology of electrospun nanofibers and textiles, Polymer, 42 (2001) 261-272.

[50] M.M. Demir, I. Yilgor, E. Yilgor, B. Erman, Electrospinning of polyurethane fibers, Polymer, 43 (2002) 3303-3309.

[51] O.S. Yördem, M. Papila, Y.Z. Menceloğlu, Effects of electrospinning parameters on polyacrylonitrile nanofiber diameter: An investigation by response surface methodology, Materials & Design, 29 (2008) 34-44.

[52] S. De Vrieze, T. Van Camp, A. Nelvig, B. Hagström, P. Westbroek, K. De Clerck, The effect of temperature and humidity on electrospinning, J Mater Sci, 44 (2009) 1357-1362.

[53] N. Nwe, T. Furuike, H. Tamura, The Mechanical and Biological Properties of Chitosan Scaffolds for Tissue Regeneration Templates Are Significantly Enhanced by Chitosan from Gongronella butleri, Materials, 2 (2009) 374.

[54] C.S. Ki, D.H. Baek, K.D. Gang, K.H. Lee, I.C. Um, Y.H. Park, Characterization of gelatin nanofiber prepared from gelatin–formic acid solution, Polymer, 46 (2005) 5094-5102.

[55] X. Yuan, Y. Zhang, C. Dong, J. Sheng, Morphology of ultrafine polysulfone fibers prepared by electrospinning, Polymer International, 53 (2004) 1704-1710.

[56] A.R. Keshtkar, M. Irani, M.A. Moosavian, Removal of uranium (VI) from aqueous solutions by adsorption using a novel electrospun PVA/TEOS/APTES hybrid nanofiber membrane: comparison with casting PVA/TEOS/APTES hybrid membrane, Journal of Radioanalytical and Nuclear Chemistry, 295 (2013) 563-571.

[57] M. Aliabadi, M. Irani, J. Ismaeili, S. Najafzadeh, Design and evaluation of chitosan/hydroxyapatite composite nanofiber membrane for the removal of heavy metal ions from aqueous solution, Journal of the Taiwan Institute of Chemical Engineers, 45 (2014) 518-526.

[58] C. Lim, E. Tan, S. Ng, Effects of crystalline morphology on the tensile properties of electrospun polymer nanofibers, Applied Physics Letters, 92 (2008) 141908.

[59] Z. Ghanavati, N. Neisi, V. Bayati, M. Makvandi, The influence of substrate topography and biomaterial substance on skin wound healing, Anatomy & Cell Biology, 48 (2015) 251-257.

[60] C.C. Berry, G. Campbell, A. Spadiccino, M. Robertson, A.S.G. Curtis, The influence of microscale topography on fibroblast attachment and motility, Biomaterials, 25 (2004) 5781-5788.

[61] H. Cao, K. Mchugh, S.Y. Chew, J.M. Anderson, The topographical effect of electrospun nanofibrous scaffolds on the in vivo and in vitro foreign body reaction, Journal of biomedical materials research Part A, 93 (2010) 1151-1159.

[62] S. Tan, R. Inai, M. Kotaki, S. Ramakrishna, Systematic parameter study for ultra-fine fiber fabrication via electrospinning process, Polymer, 46 (2005) 6128-6134.

[63] S.H. Teng, E.J. Lee, B.H. Yoon, D.S. Shin, H.E. Kim, J.S. Oh, Chitosan/nanohydroxyapatite composite membranes via dynamic filtration for guided bone regeneration, Journal of Biomedical Materials Research Part A, 88 (2009) 569-580.

[64] S. Tavakol, M.R. Nikpour, A. Amani, M. Soltani, S.M. Rabiee, S.M. Rezayat, P. Chen, M. Jahanshahi, Bone regeneration based on nano-hydroxyapatite and hydroxyapatite/chitosan nanocomposites: an in vitro and in vivo comparative study, J Nanopart Res, 15 (2012) 1-16.

[65] M. Leedy, H. Martin, P.A. Norowski, J.A. Jennings, W. Haggard, J. Bumgardner, Use of Chitosan as a Bioactive Implant Coating for Bone-Implant Applications, in: R. Jayakumar, M. Prabaharan, R.A.A. Muzzarelli (Eds.) Chitosan for Biomaterials II, Springer Berlin Heidelberg2011, pp. 129-165.

[66] F.J. Pavinatto, L. Caseli, O.N. Oliveira, Chitosan in Nanostructured Thin Films, Biomacromolecules, 11 (2010) 1897-1908.

[67] J.P. Chen, S.H. Chen, G.J. Lai, Preparation and characterization of biomimetic silk fibroin/chitosan composite nanofibers by electrospinning for osteoblasts culture, Nanoscale Res Lett, 7 (2012) 170.

[68] M. Hasegawa, A. Isogai, F. Onabe, M. Usuda, R.H. Atalla, Characterization of cellulose–chitosan blend films, J. Appl. Polym. Sci., 45 (1992) 1873-1879.

[69] M. Jevtić, A. Radulović, N. Ignjatović, M. Mitrić, D. Uskoković, Controlled assembly of poly(d,l-lactide-co-glycolide)/hydroxyapatite core–shell nanospheres under ultrasonic irradiation, Acta Biomater, 5 (2009) 208-218.

[70] L.C. Mendes, G.L. Ribeiro, R.C. Marques, In situ hydroxyapatite synthesis: Influence of collagen on its structural and morphological characteristic, Mater. Sci. Appl., 3 (2012) 580-586.

[71] S. Meejoo, W. Maneeprakorn, P. Winotai, Phase and thermal stability of nanocrystalline hydroxyapatite prepared via microwave heating, Thermochimica Acta, 447 (2006) 115-120.

[72] C.G.T. Neto, J.A. Giacometti, A.E. Job, F.C. Ferreira, J.L.C. Fonseca, M.R. Pereira, Thermal Analysis of Chitosan Based Networks, Carbohydrate Polymers, 62 (2005) 97-103.

[73] K. Webb, V. Hlady, P.A. Tresco, Relative importance of surface wettability and charged functional groups on NIH 3T3 fibroblast attachment, spreading, and cytoskeletal organization, Journal of biomedical materials research, 41 (1998) 422-430.

[74] S. Sista, C. Wen, P.D. Hodgson, G. Pande, Expression of cell adhesion and differentiation related genes in MC3T3 osteoblasts plated on titanium alloys: role of surface properties, Materials Science and Engineering: C, 33 (2013) 1573-1582.

[75] D. Verma, K.S. Katti, D.R. Katti, Osteoblast adhesion, proliferation and growth on polyelectrolyte complex–hydroxyapatite nanocomposites, Philosophical Transactions of the Royal Society of London A: Mathematical, Physical and Engineering Sciences, 368 (2010) 2083-2097.

[76] X. Yang, X. Chen, H. Wang, Acceleration of osteogenic differentiation of preosteoblastic cells by chitosan containing nanofibrous scaffolds, Biomacromolecules, 10 (2009) 2772-2778.

[77] P.P.K. Normalizacyjny, Biological Evaluation of Medical Devices - Part 5: Tests for in Vitro Cytotoxicity (ISO 10993-5:2009), Polski Komitet Normalizacyjny2009.

[78] P. Wutticharoenmongkol, P. Pavasant, P. Supaphol, Osteoblastic Phenotype Expression of MC3T3-E1 Cultured on Electrospun Polycaprolactone Fiber Mats Filled with Hydroxyapatite Nanoparticles, Biomacromolecules, 8 (2007) 2602-2610.

[79] C.D. Hoemann, H. El-Gabalawy, M.D. McKee, In vitro osteogenesis assays: Influence of the primary cell source on alkaline phosphatase activity and mineralization, Pathologie Biologie, 57 (2009) 318-323.

[80] C. Zhang, H. Yuan, H. Liu, X. Chen, P. Lu, T. Zhu, L. Yang, Z. Yin, B.C. Heng, Y. Zhang, H. Ouyang, Well-aligned chitosan-based ultrafine fibers committed teno-lineage differentiation of human induced pluripotent stem cells for Achilles tendon regeneration, Biomaterials, 53 (2015) 716-730.

LIST OF TABLES

Table 1 *- Electrospun samples obtained under different electrospinning parameters: A-Ch, B-Ch, C-ChHa e D-ChHa*

Solution	***Parameters***	***Specimen***
(Ch)	*0.3 mLh^{-1}-12 cm-10 kV(A)*	*A-Ch*
(Ch)	*0.3 mLh^{-1}-15 cm-10 kV(B)*	*B-Ch*
(ChHa)	*0.5 mLh^{-1}-12 cm-17 kV(C)*	*C-ChHa*
ChHa)	*0.5 mLh^{-1}-15 cm-17 kV(D)*	*D-ChHa*

Table 2 *- Weight loss stages associated with the evaporation of water absorbed / adsorbed and decomposition obtained by TG and dTG*

Sample	***1º Stage (water loss)***	***2º Stage (decomposition)***	***3º Stage (decomposition)***
Chitosan	*25-168 ºC →5.04 %*	*202-433 ºC →35.99 %*	-
Electrospun Ch	*25-118 ºC →9.04 %*	*126-280 ºC →40.06 %*	*280-431ºC →24.03 %*
Electrospun ChHa	*25-120 ºC →10.90 %*	*125-288 ºC →40.15 %*	*288-435 ºC →21.47 %*

FIGURES

Figure 1 *- SEM images of the electrospun products from A-Ch, B-Ch, C-ChHa and D-ChHa*

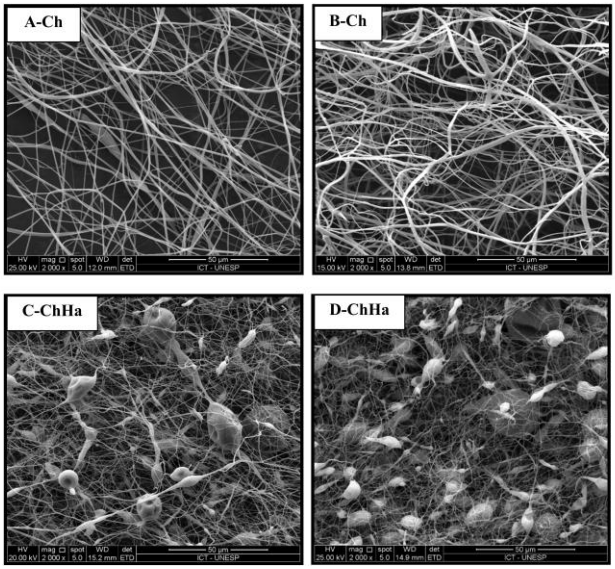

Figure 2 *- Average fibers diameter histograms: A-Ch, B-Ch, C-ChHa and D-ChHa.*

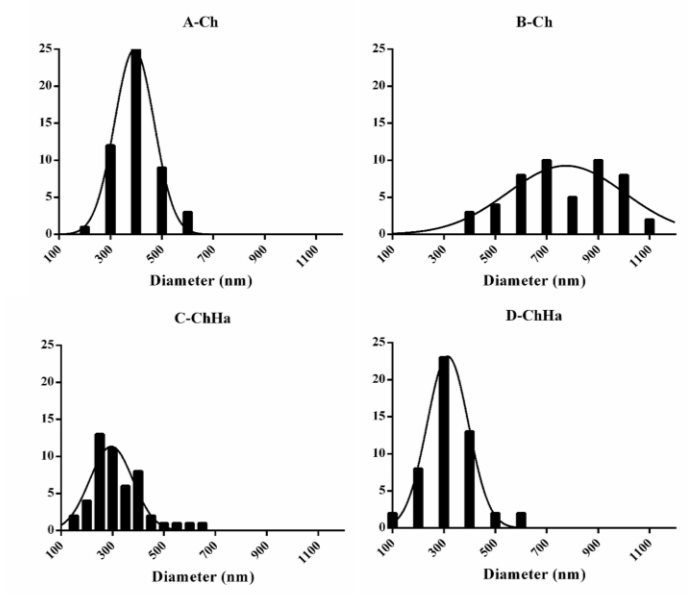

Figure 3 *- A-Ch, B-Ch, C-ChHa and D-ChHa profilometry analysis in 2D and 3D images*

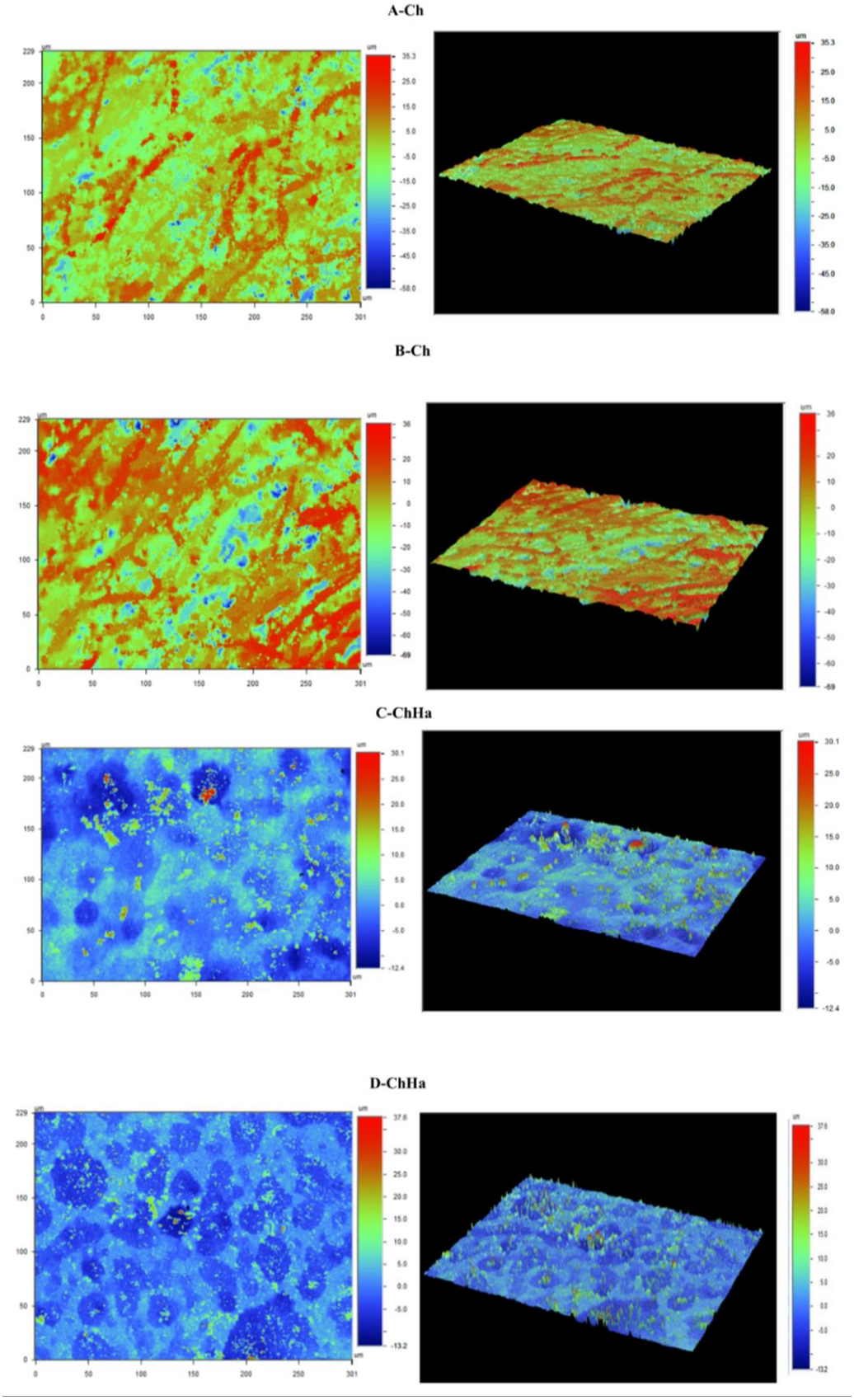

Figure 4 *– AFM analysis A: Electrospun Ch AFM analysis and B: Electrospun ChHa*

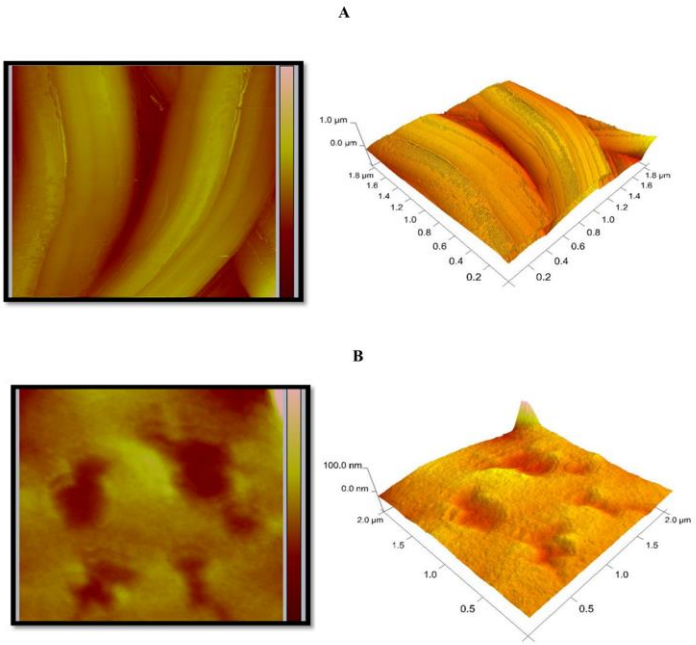

Figure 5 *– A) FTIR analysis of all samples B) Characteristic bands from Ch and ChHa and C) Characteristic bands from nHAp*

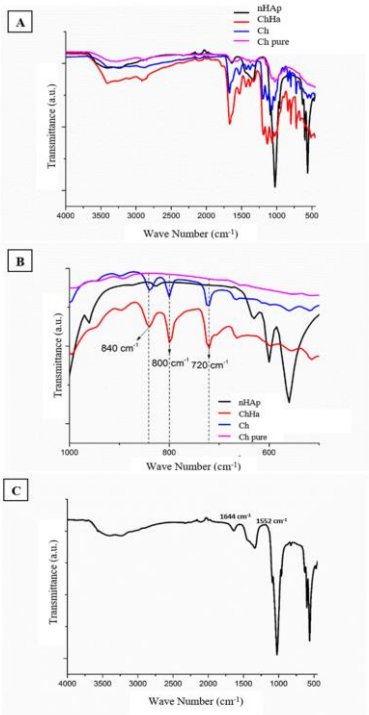

Figure 6 *- (a) TG curves and (b) dTGs samples of Ch, electrospun Ch, electrospun ChHa and nHAp.*

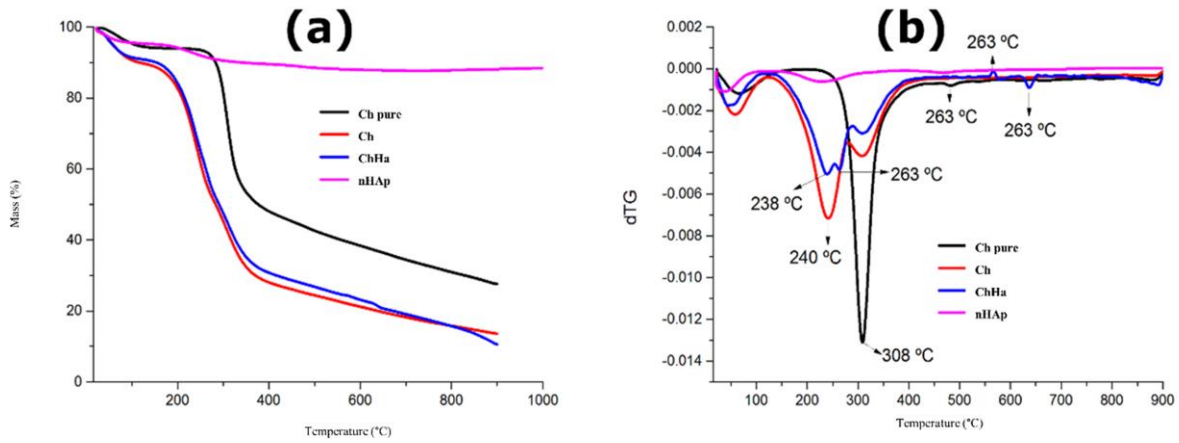

Figure 7 *- Measurement of cell viability MTT assay*

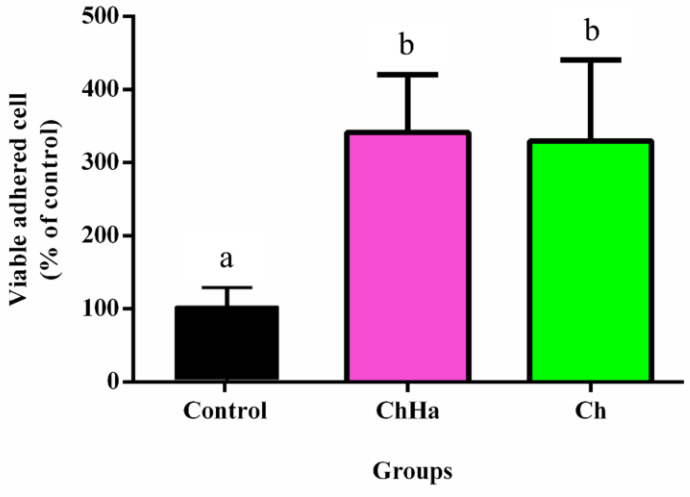

Figure 8 *– Osteogenic differentiation by Alkaline phosphatase activity of MSCs cells after 10 days of incubation on control group, Chitosan samples (Ch) and chitosan / nHAp samples (ChHa). Values are reported as mean ± SD (n = 5).*

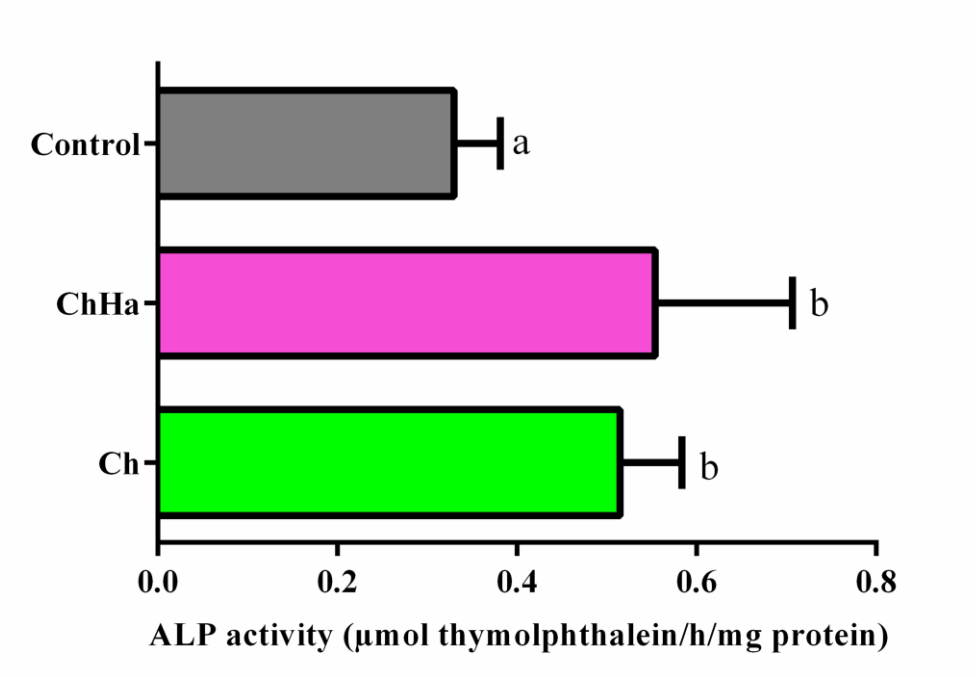

Graphical Abstract

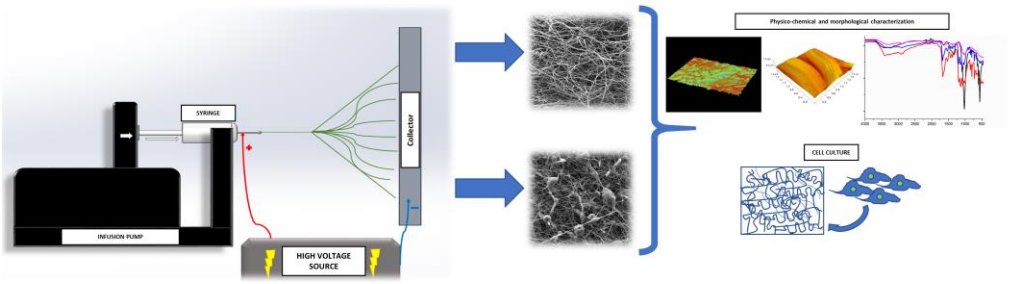

2.2 Artigo – Sato TP, Mello DCR, Vasconcellos LMR, Valente AJM, Borges ALS. Desenvolvimento de matrizes de hidrogel de quitosana-DNA e quitosana-pectina para sistema de entrega de fitoterápicos / *Development of Chitosan-DNA and Chitosan-Pectin hydrogel matrices for herbal medicine delivery system**

RESUMO

Este estudo teve como objetivo sintetizar hidrogéis de quitosana-DNA (CS-DNA) e quitosana-pectina (CS-P) para administração de fitoterápicos. Para isso, os hidrogéis foram preparados pela técnica de emulsão (óleo em água): as emulsões foram obtidas pela mistura da fase aquosa da solução de CS (1 mL) e solução de DNA (1 mL) (1:1 razão de quitosana:DNA) ou Solução de P (1 mL) (1:1 razão de quitosana:pectina) com álcool benzílico (5 mL) usando um instrumento de dispersão de alto desempenho. O Própolis Verde (PV) foi incorporado por embebição: 20 mg hidrogel numa solução aquosa de PV (70 µg/mL) por 2h e a cinética de liberação do PV foi analisada a 25 e 37 ºC em água e saliva artificial. Os espécimes obtidos foram liofilizados e depois caracterizados utilizando diferentes técnicas e a viabilidade celular *in vitro* foi realizada utilizando a linha celular MG63. A presença de pectina foi evidenciada pela ocorrência de uma forte banda a 1745 cm^{-1}, também ocorrendo na mistura, atribuída aos grupos esterificados. As bandas que ocorrem em 1105 e 1010 cm^{-1}, na região das impressões digitais, são típicas dos polímeros de pectina e podem ser atribuídas ao alongamento C=O. Nos géis de DNA e CS-DNA, é possível observar uma forte banda a 1650 cm^{-1}, atribuída à vibração de estiramento C2=O2 da citosina. A sorção de PV induziu uma modificação significativa da morfologia da superfície do gel. A partir do TGA, pode-se concluir que ocorre alguma separação de fases entre a quitosana e o DNA. A eficiência do encapsulamento não muda significativamente com a temperatura. A cinética de liberação na água ou na saliva segue um mecanismo de duas etapas. E os resultados biológicos exibiram que esses materiais são aceitáveis no ambiente biológico e podem fornecer evidências para o potencial de material biomimético. Pode-se concluir que a complexação de hidrogel de CS com DNA e pectina é uma alternativa viável ao sistema de administração de medicamentos à base de plantas como o PV.

Palavras-chave: Hidrogel. Quitosana. Pectina. DNA. Própolis.

---

*Artigo elaborado de acordo com as normas do Periódico *Journal of Biomaterials Applications* (*Print version* ISSN 0885-3282).

ABSTRACT

This study aimed to synthesize Chitosan-DNA (CS-DNA) and Chitosan-Pectin (CS-P) hydrogels for drug delivery of herbal medicine. For this, hydrogels were prepared by emulsion technique (oil-in-water): emulsions were obtained by mixing aqueous phase of the Ch solution (1 mL) and DNA solution (1 mL) (1:1 ratio of Chitosan:DNA) or Pectin solution (1 mL) (1:1 ratio of Chitosan:Pectin) with benzyl alcohol (5 mL) using a high-performance dispersing instrument. Green Propolis (GP) was incorporated by imbibition: 20mg of hydrogel in 70 µg/mL GP aqueous solution for 2h and GP release kinetics was analyzed at 25 and 37ºC in water and simulated saliva. The obtained specimens were freeze-dried and then characterized using different techniques and in vitro cell viability was performed using MG63 cell line. The presence of pectin was evidenced by the occurrence of a strong band at 1745 cm^{-1}, also occurring in the blend, ascribed to esterified groups. The bands occurring at 1105 and 1010 cm^{-1}, in the finger-print region are typical of pectin polymers and can be attributed to the C=O stretching. In the DNA and chitosan-DNA gels it is possible to observe a strong band at 1650 cm^{-1}, slightly shifted from the chitosan band, assigned to the C2=O2 stretching vibration of cytosine. The sorption of GP induced a significant modification of the surface morphology of the gel. From TGA it can be concluded that some phase separation occurs between chitosan and DNA. The encapsulation efficiency does not significantly change with temperature. The release kinetics either in water or saliva follow a two-step mechanism. And the biological results exhibited that these materials are acceptable in the biological environment and can provide evidence for the potential of biomimetic material. It can be concluded that the hydrogel complexation of CS with DNA and Pectin is a viable alternative to drug delivery system of herbal medicine such as GP.

Keywords: Hydrogel. Chitosan. Pectins. DNA. Propolis.

INTRODUCTION

Hydrogels are known as crosslinked polymeric 3D networks capable of absorbing and retaining large amounts of water or biological fluids [1 2], having a microstructure similar to the extracellular matrix (ECM) [2] and a biocompatibility to blood and biological tissues [3]. Besides, hydrogels can be

designed with responsive properties which make them highly appreciated for biomedical and pharmaceutical (drug/gene deliver) applications [4-7].

Thus, much effort has been made on the hydrogel-based matrices for the development of vectors for the delivery of active substances for different targets. Among different strategies, the use of biopolymers is mandatory. Following such approach, chitosan (Chi) is a cationic biopolymer, obtained from the chitin desacetylation of crustaceous exoskeleton [8], showing antimicrobial biodegradable and biocompatible properties. Furthermore, due to the presence on its structure of amine and hydroxyl groups [9, 10], the Chit is highly chemically versatile, being used for several applications in pharmaceutical and medical areas [11], especially for wound healing applications [12] as they are similar to the natural extracellular matrix (ECM).

The dissolution of chitosan occurs in slightly acidic (pH < 6.5) aqueous solutions, as a consequence of the protonation of its amine groups, allowing the formation of either chemical or physical crosslinked hydrogels [13]. Covalently crosslinked chitosan hydrogels are very effective in drug delivery systems [14, 15]; however, they may show some drawbacks as, for example, the use of toxic crosslinkers or initiators. The use of physical hydrogels allow to overcome such limitation [16]. Among different approaches, and taking advantage of the positively charged chitosan, we have decided to investigate the formation of chitosan-DNA and chitosan-pectin coacervate hydrogels. Deoxyribonucleic acid (DNA) is a biopolymer composed of deoxyribose sugar, able to carry genetic information [17]. DNA hydrogels have unique properties such as biocompatibility, selective binding, and molecular recognition [18, 19], creating a wide range of potential applications in drug delivery [6, 20] and tissue engineering [21-23]. In fact, among biological polyelectrolytes, DNA has always attracted particular interest, and there are numerous studies of the interactions between DNA and polycations [24-27]. The formation of coacervate hydrogels is achievable once DNA

is completely ionized at neutral pH [28] enabling the interaction with positively charged molecules, such as chitosan [29].

Pectin (P) is another polianion at pH higher than ca. 9 that can form coacervate hydrogels with chitosan [30, 31]. Pectin is a plant cell wall polysaccharide used as a gelling and stabilizing polymer in food or biomedical products due the influence on human health such as cholesterol levels and local bleeding [32, 33].

These two matrices were tested as a sustained drug release matrix for Green Propolis (GP). This is an herbal medicine produced by Apis mellifera honeybees, from Baccharis dracunculifolia DC (Asteraceae), and used as anti-inflammatory [34], antifungal [35] and antioxidant [36, 37] drug, due to its high levels of phenolic acids [38].

MATERIALS AND METHODS

Materials

Chitosan with acetylation degree of 15 mol% (M_w: 87 × 10^3 g mol^{-1}) was purchased from Golden-Shell Biochemical (China). Pectin from citrus peel and double-stranded (ds) DNA (sodium salt from salmon testes), with a polymerization average degree of ca. 2000 base pairs, were purchased from Sigma. Benzyl alcohol (99%) was obtained from Merck KGaA (Germany).

Aqueous extract of Green Propolis was obtained from Apis Flora (Ribeirão Preto, SP, Brazil). Millipore-Q water has been used to prepare the solutions.

Simulated saliva was made by Indiana University modified method [39], prepared according to Fusayama et al (1963) [40].

Hydrogels preparation

Both cocervate hydrogels (chitosan-DNA and chitosan-pectin) have been prepared by emulsion technique (oil-in-water). The preparation of the former gel has been done using an acetate buffer (pH 6). This buffer was chosen to balance the cationic density of chitosan and the chemical instability of DNA [41].

Thus, a chitosan aqueous solution (1 % w/v) was initially prepared in acetate buffer and then filtered through a paper filter to remove insoluble substances [31]. DNA and pectin aqueous solutions were prepared in phosphate buffer at pH 6 and pH 9.2, respectively, under stirring for 12 hours, at room temperature. The emulsions were obtained by mixing aqueous phase of the Ch solution (1 mL) and DNA solution (1 mL) (1:1 (v/v) ratio of Ch:DNA) or Pectin solution (1 mL) (1:1 (v/v) ratio of Ch:Pectin) with benzyl alcohol (5 mL) using a Ultra-Turrax at 31-34000 rpm min^{-1} for 5 minutes [42].

Hydrogel Characterization

The synthesized hydrogels were freeze-dried previously to their characterization by different techniques. Attenuated reflection infrared spectroscopy (ATR-FTIR) was carried out in a Varian Cary 630 FTIR Spectrometer, with wavenumber ranging from 650 to 4000 cm^{-1}.

The thermogravimetric analysis (TGA) were performed in a thermogravimetric analyzer (TG209 F3 Tarsus Netzsch Instruments). Samples of ca. 5 mg were weighed in alumina pans and heated from 25 ºC to 800 ^{o}C at a 10 ^{o}C min^{-1} rate, under N_2 atmosphere (20 mL min^{-1}).

The surface morphologies of hydrogels have been analyzed by scanning electron microscopy (SEM) with a JEOL model 5310 scanning microscope operating under low vacuum at 15 kV. The membranes were submitted to a fast cryogenic treatment by diving gel samples into liquid nitrogen for 10 s, and then they were left overnight in a freeze dryer (Free Zone 4.5-Labconco) before being coated with a gold film.

The effect of water and simulated fluids on hydrogels before and after the loading of Green Propolis was assessed by swelling degree (Q). Different samples of the same membrane were cut, weighed, and immersed in water or simulated solutions and left to reach the swelling equilibrium (2days). After this time, membranes were removed from the solution, any drops of solution were wiped off, then the weight of the membrane was measured using an analytical balance (ADA 120LE, (0.1 mg). Each experiment was repeated twice. The swelling degree of the gel (Q) was calculated by using the equation

$$Q = \frac{m_w}{m_x} \qquad (1)$$

where m_w and m_x are the masses of water (or solution) in the swollen gel and in the xerogel, respectively. The mass of xerogel samples has been obtained using the weight of the sample after synthesis and taking into account the solid content of the gel [43].

Loading and release of Green Propolis

Green Propolis has been incorporated into coacervate gels by imbibition. A 70µg/mL GP aqueous solution was prepared; after that, hydrogel samples (of ca. 20 mg) were placed in that volume of GP solution and left there for 2 hours, at 25 ºC, using a thermostatic bath.

The encapsulation (EE) efficiency was calculated by using, respectively, the following equations:

$$EE = \frac{\left(\text{total amount of GP} - \text{non-bound GP}\right)}{\text{total amount of GP}} \times 100 \qquad (2)$$

To determine the GP release kinetics the hydrogels samples, after GP encapsulation, were placed in vessels containing 20 mL of water, and kept in an incubator (Labwit, ZWY-100H), at 37 ºC and 150 rpm. At predetermined time intervals (20 min), an aliquot of the supernatant were taken from the vessel and

storage for GP quantification. Meanwhile, that volume was replaced by water. The process was repeated until the release equilibrium is attained. The GP released into the supernatant was quantified spectrophotometrically by measuring the absorbance at range of 200 to 800nm using a double-beam Shimadzu UV-2100 spectrometer (SHI-MADZU EUROPA, Germany).

Biological Analysis

In this present study were used established lineage of osteoblast-like cells (MG63) acquired from Rio de Janeiro Cell Bank (Rio de Janeiro, RJ, Brazil). Cells were cultured in Modified Eagle´s medium (Life Technologies, NY, USA) containing 10 % fetal bovine serum (Life Technologies, NY, USA) and penicillin (100U/mL) at 37 C in a humidified atmosphere of 5 % CO_2. The culture medium was changed to each two days until moment test. All tests were performed according to ISO 10993 guidelines, with three independent experiments.

Initially, five samples for each material were placed into 24 well plates (TPP, Curitiba, Brazil), and followed 2 x 10^4 cells were placed in each well. After 7 days for cultured, MTT colorimetric assay were performed with incubation in 3-(4,5-dimethylthiazol-2-yl)-2,5-diphenyltetrazolium bromide (Sigma-Aldrich St Louis MO, USA), then the cells were lysed with a propanol acid solution (Sigma-Aldrich St Louis MO, USA) for colorimetric measurement in a spectrophotometer (EL 808 BioTek Instruments, Winooski, USA) at 570 nm, as previously describe [44]. The values were expressed in percentage of viable cells compared to the control group (only cells) considered 100%.

Proteins were extracted with 0.1 % sodium dodecyl sulfate (Sigma-Aldrich St Louis MO, USA), followed by addition of Lowry solution (Sigma-Aldrich St Louis MO, USA). The extract was diluted in Folin–Ciocalteu reagent (Sigma-Aldrich St Louis MO, USA) and the absorbance was assessed in a spectrophotometer (8582 Micronal, São Paulo, Brazil) at 680 nm [44]. The total

protein content was calculated from a bovine serum albumin standard and expressed in μg/mL.

RESULTS AND DISCUSSION

Gels characterization

Figures 1 and 2 show the FTIR spectra of the chitosan-pectin and chitosan-DNA blend hydrogels, respectively, and the corresponding isolated polymers. The IR spectra of chitosan (Figures 1 and 2) show two characteristic bands at 1648 and 1538 cm^{-1} assigned to (C=O) stretching mode and N-H bending of amide group. A band at 1378 cm^{-1} can be attributed to the -CH_3 symmetrical deformation and the strong band at 1076 cm^{-1} characterizes the C-O stretching [45, 46]. Furthermore, the spectra show bands at 3417 cm^{-1} that indicates dimeric O-H stretch and at 1425 cm^{-1} indicating aromatic C-C stretch [47].

To confirm the occurrence of the coacervation process, the presence of pectin was evidenced by the occurrence of a strong band at 1745 cm^{-1}, also occurring in the blend, ascribed to esterified groups, and at 1624 assigned to free carboxyl groups [48]. The bands occurring at 1105 and 1010 cm^{-1}, in the finger-print region are typical of pectin polymers and can be attributed to the C=O stretching [31, 49].

In the DNA and chitosan-DNA gels it is possible to observe a strong band at 1650 cm^{-1}, slightly shifted from the chitosan band, assigned to the C2=O2 stretching vibration of cytosine [43]; the shoulder found at the blend and at DNA gels, at 1590 cm^{-1}, can be attributed to a couple of C6=O6, C5-C6, and C4=C5 stretching vibrations of guanine [50]. The small modifications of the FTIR spectra around 1590 cm^{-1} may suggest a different base-pairing pattern of DNA alone and in the blend [43]. Further bands, in the CHD spectrum, at 526 cm^{-1} and 890 cm^{-1}, the later only observed in the DNA-containing gels, indicate the deoxyribose region [51], and the deoxyribose-phosphate groups [52].

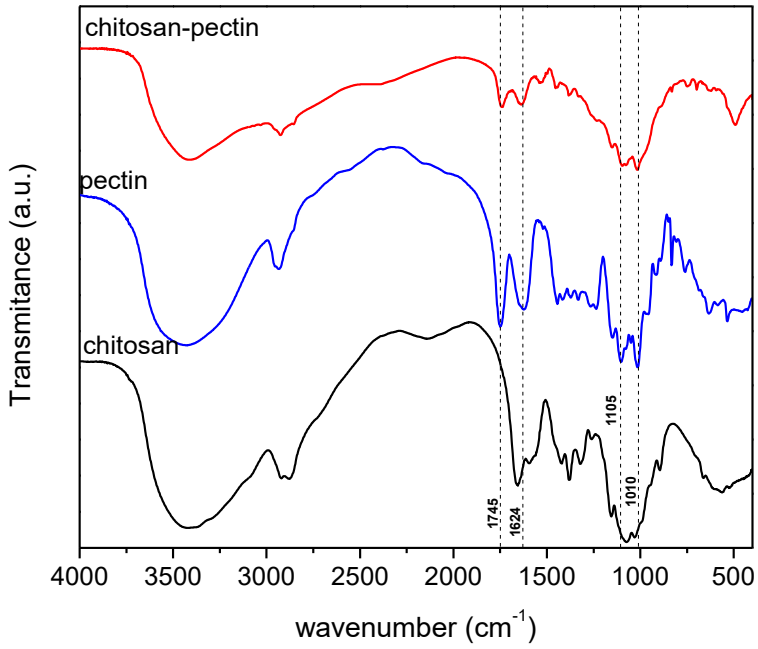

Figure 1. *Infrared spectra of chitosan, pectin and the chitosan-pectin blend gel.*

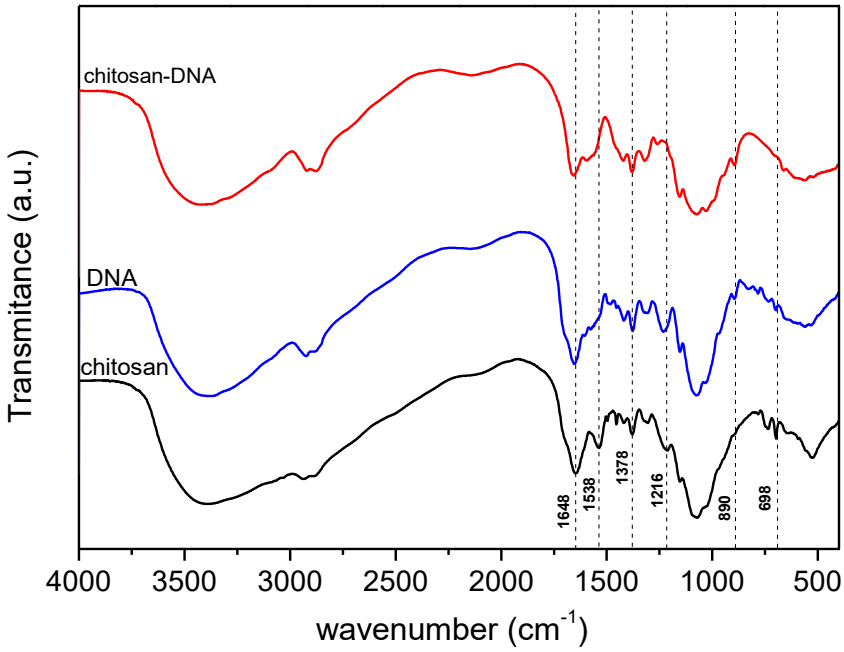

Figure 2. *Infrared spectra of chitosan, DNA and the chitosan-DNA blend gel.*

The gels have also been characterized by thermogravimetric analysis (Figures 3 and 4). To have an assessment on the main degradation temperatures, the maximum degradation rate has been computed (dTG), and the corresponding temperature, T_{max}, obtained. In the Figure 3, and excluding the T_{max} obtained at temperatures below 150 ºC, caused by the evaporation of residual water, two main degradation steps at 234 ºC and 292 ºC were found for pectin [53, 54] and chitosan [55], respectively. It is interesting that for the chitosan-pectin blend two degradation steps can be found at 227 ºC and a 548 ºC; the latter can be justified by the degradation of chitosan. The former maximum degradation temperature, corresponding to ca. 63% weight loss, occurs at temperature below the main transition steps for single pectin and chitosan. This can be justified by a decrease in the thermal stability of blend as a consequence of ionic interactions between pectin and chitosan, leading to a plasticizer-like effect.

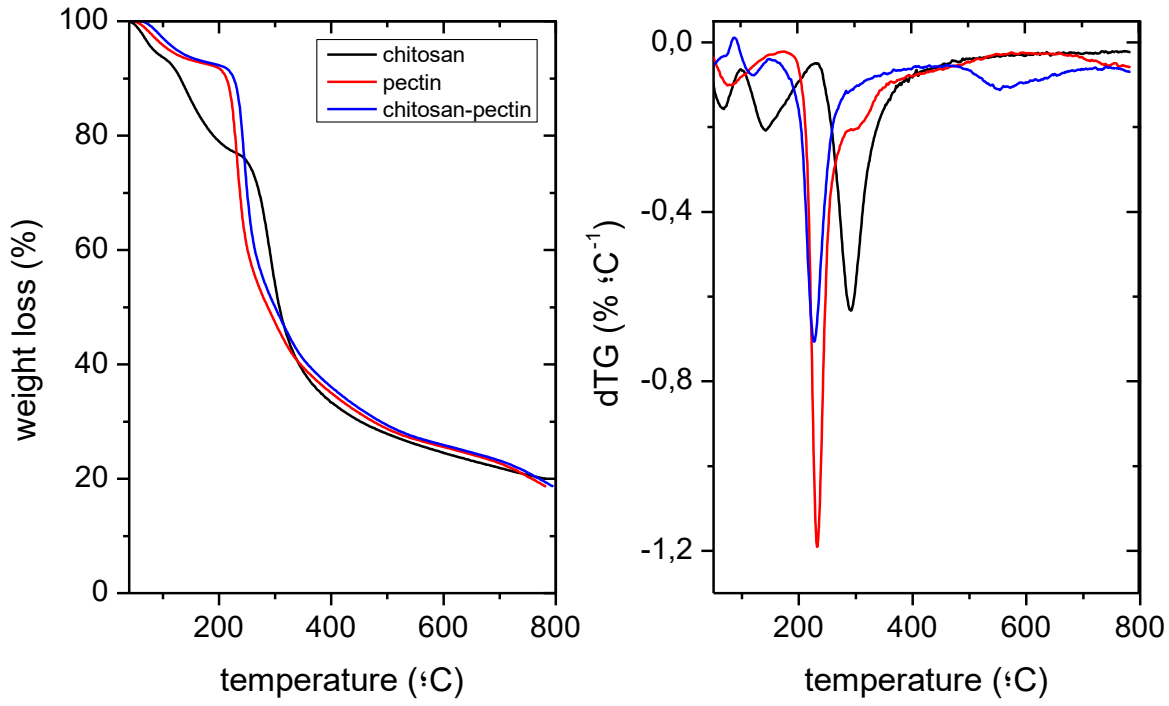

Figure 3. *TGA and dTG curves of CS (—), Pec (—) and CS-Pec (—).*

Figure 4. *TGA and dTG curves of chitosan (—), DNA (—) and chitosan-DNA (—).*

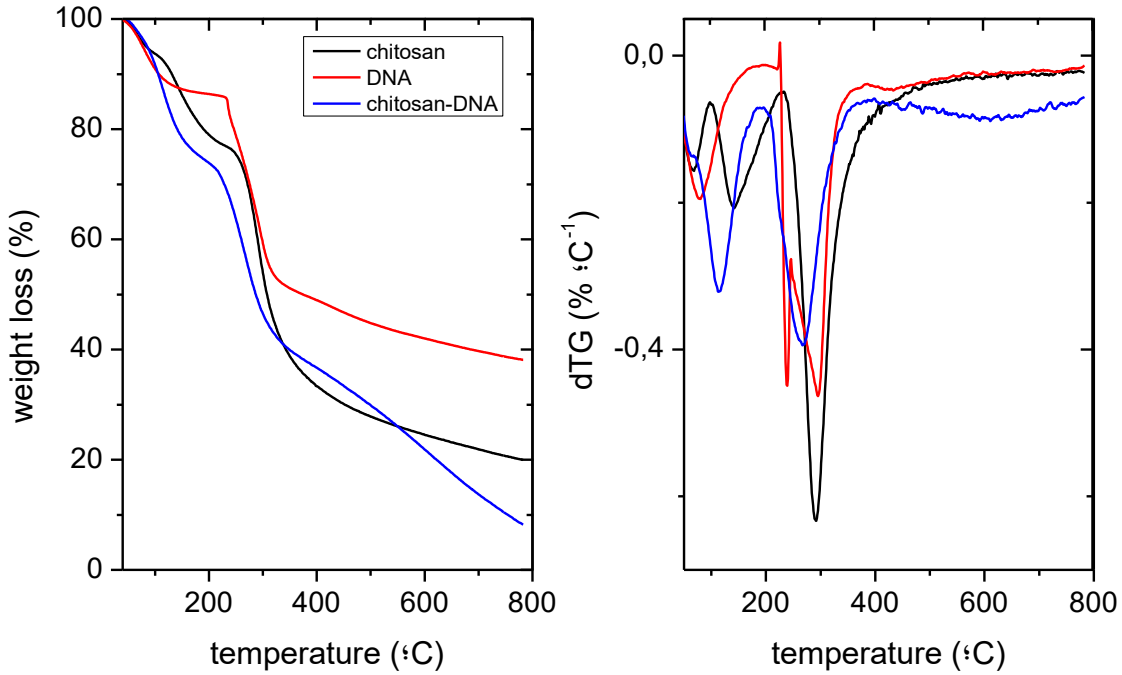

The analysis of figure 4 shows that the first degradation step of DNA occurs at 238 ºC [56], followed by a second degradation step at 295 ºC, suggesting that the presence of different secondary structures might be present. However, the most remarkable difference between this blend, and the chitosan-pectin one, is that the main degradation step occurs at 268 ºC, suggesting a higher degree of phase separation.

From the analysis of the surface morphology of chitosan-pectin and chitosan-DNA gels (Figure 5), it can be observed that the surface of the latter shows a more heterogeneous structure, characterized by well-defined aggregates and fiber-like structures. On the other hand, for chitosan-pectin the surface morphology is more featureless, non-porous structure, indicating some irregularities that might be related with some phase separation. This morphology can increase stability by providing higher resistance [57]. However, after the GP sorption a significant change in the surface morphology of

chitosan-DNA is observed; i.e., the surface becomes highly porous. This has been reported for other DNA-containing composites, such as PVA-DNA [43], and suggests that the GP has a significant effect or even interaction with the polymers. This might also justify the lowest amounts of GP release by chitosan-DNA (see the discussion below), when compared with the chitosan-pectin, despite its higher porosity. However, the surface of chitosan-pectin does not undergo relevant modification upon GP loading, indicating that the pectin is playing a major role [58].

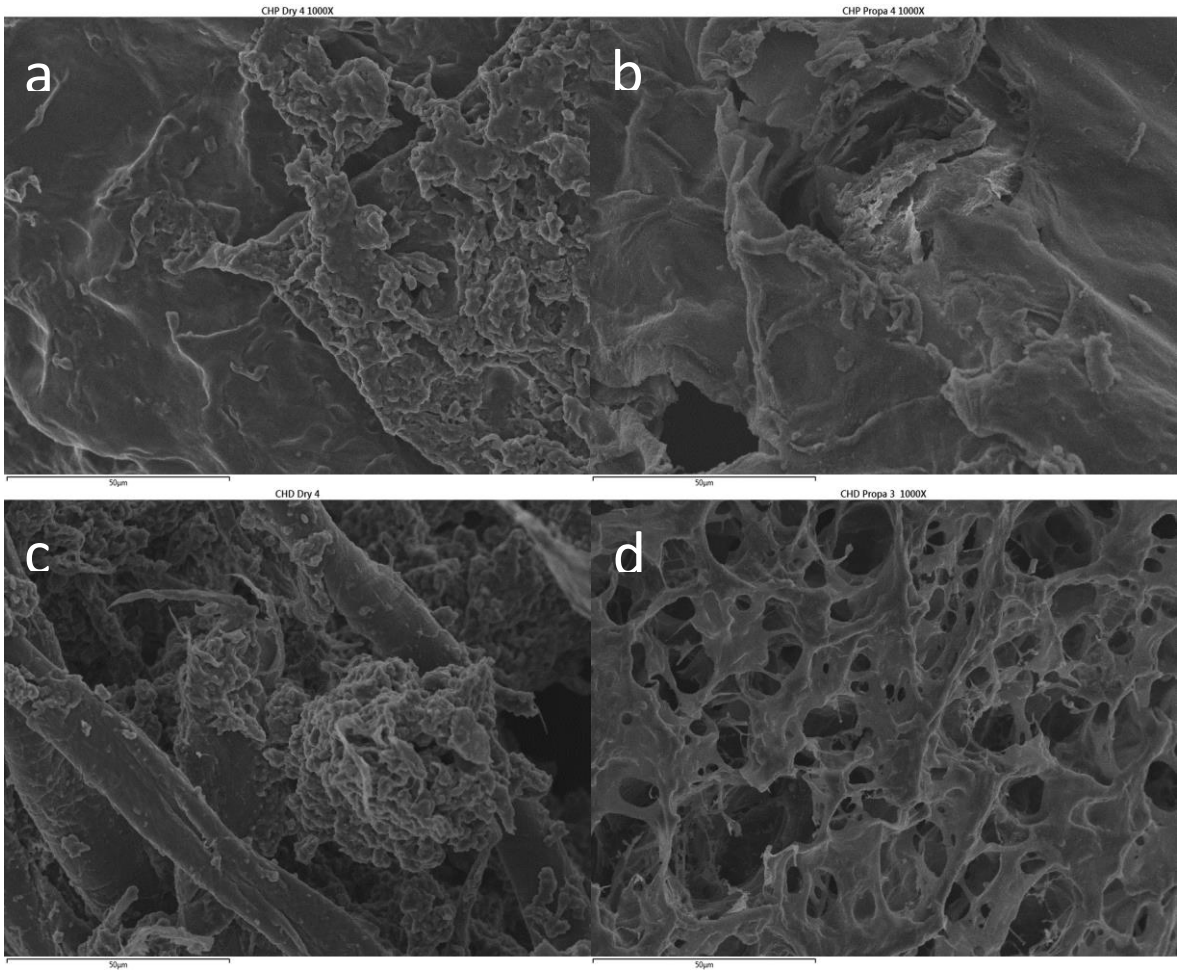

Figure 5. *Scanning electron micrographs of chitosan-pectin (a, b) and chitosan-DNA (c,d) before (a,c) and after (b,d) GP loading. ×1000 magnification. Scale = 50 □m.*

Loading and Drug release

Table 1 shows the encapsulation efficiency of GP into chitosan-pectin and chitosan-DNA blend gels. It can be seen that the EE in the chitosan-DNA is significant lower (ca. 3.5 fold lower) than those obtained for chitosan-pectin. This might be related with the occurrence of higher phase separation in the chitosan-DNA gel and also the lower swelling degree of this gel (Q=700 %) when compared with that for chitosan-pectin (Q=1109%). However, it is surprising that the cumulative release, in percentage, in higher for the chitosan-DNA gel. This might be due to the change in the structure of pectin-DNA gel, becoming a more porous surface structure (see Figure 5). In any case, the absolute value of the maximum released amount of GP is always higher for chitosan-pectin.

Table 1. *Encapsulation efficiency and cumulative release of GP in chitosan-pectin and chitosan-DNA coacervate gels, at 25ºC.*

	Chitosan-pectin		*Chitosan-DNA*	
	25 ºC	*37 ºC*	*25 ºC*	*37 ºC*
		Water		
EE (%)	*19*	*21*	*7*	*8*
Cumulative release (%)	*13.2*	*12.1*	*25.7*	*30*
		simulated saliva		
EE (%)	*30*	*38*	*8*	*10*
Cumulative release (%)	*13.9*	*19.9*	*31.6*	*36.5*

Figures 6 and 7 show the release profiles of Green Propolis from chitosan-pectin and chitosan-DNA gels, respectively, to simulated saliva at 25 and 37 ºC.

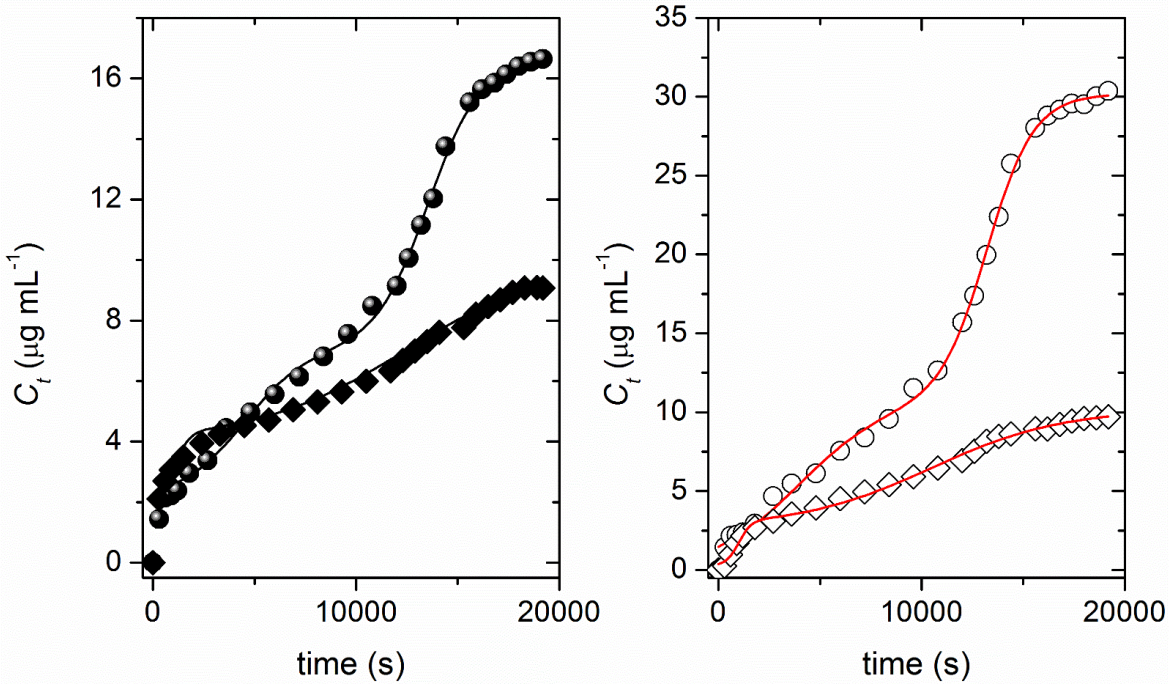

Figure 6. *Release kinetics of GP from chitosan-pectin gels to water (diamond) and simulated saliva (spheres), at 25 and 37 ºC (black and white data points, respectively). Solid lines were obtained by fitting eq. (3) to the experimental data.*

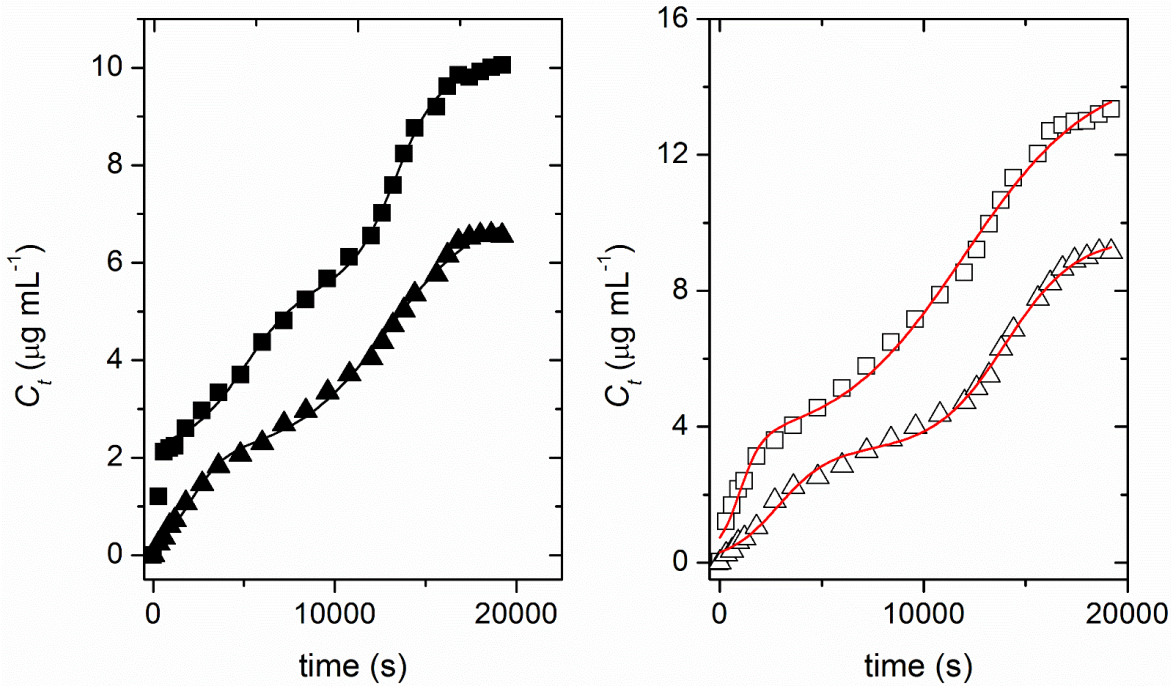

Figure 7. *Release kinetics of GP from chitosan-DNA gels to water (triangle) and simulated saliva (square), at 25 and 37 ºC (black and white data points, respectively). Solid lines were obtained by fitting eq. (3) to the experimental data.*

As a first approach we can observe that in all cases the release kinetics does follow a two-step mechanism; however, it is also clear that such a mechanism occurs concomitantly once no plateau is observed just before the beginning of the 2nd significant release – this will be discussed later. Two other points are worth noticing: the cumulative release increase by increasing the temperature (the exception occurs for the release from chitosan-pectin to water), being more significant in the case of chitosan-pectin gel; and at 25 ºC a boost release can be observed during the first 10 minutes release. The later process might be justified by a surface phenomenon (either surface erosion or preferential adsorption) [59]*; however, that process is somewhat hindered by increasing the temperature and, consequently, the origin of mass transport becomes not relevant.*

In order to have a better insight on the release mechanism several heuristic models have been tested (e.g., Weibull, Logistic, Korsmeyer-Peppas and Peppas-Sahlin [60-62] without success – results not shown. However, assuming that the release is characterized by a biphasic release that may occurs simultaneously, as can be inferred from the continuous increase of the GP as a function of time (i.e., no two plateaus of cumulative release concentration as a function of time are observed), the following equation has been used [63]:

$$C_t = C_0 + \left(C_{eq} - C_0\right)\left(\frac{p}{1+10^{(\log t_1 - t)k_1}} + \frac{1-p}{1+10^{(\log t_2 - t)k_2}}\right) \qquad (3)$$

where C_0, C_t and C_{eq} are the initial, cumulative and equilibrium release concentrations of GP, respectively, $logt_1$ and $logt_2$ correspond to the first and second EC_{50} (i.e. the concentrations of the drug that gives half-life response) and p is the contribution of each phase for the whole release profile. All the fitting parameters, summarized in the Table 2, have been estimated through a least-squares method, with a confidential degree of 95%, by using Origin 8.5 software, and keeping C_0 as constant and equal to zero.

Table 2. *Fitting Parameters of eq.3 to experimental release data of GP Loaded into chitosan-pectin and chitosan-DNA gels to simulated saliva, at 25 and 37 ºC.*

	Chitosan-pectin		*Chitosan-DNA*	
	25ºC	*37ºC*	*25ºC*	*37 ºC*
		Water		
C_{eq} / (□g mL^{-1})	*10.1 (±0.4)*	*10.2 (±0.3)*	*7.2 (±0.2)*	*9.6 (±0.2)*
$logt_1$ /s	*1051 (±73)*	*1005 (±74)*	*2051 (±203)*	*2851 (±214)*
$logt_2$ / s	*12571 (±390)*	*10460 (±360)*	*12878 (±242)*	*14005 (±158)*
k_1 /s^{-1}	*1.2 (±0.3)×10^{-3}*	*1.5 (±0.5)×10^{-3}*	*4.7 (±0.2)×10^{-4}*	*3.5 (±0.4)×10^{-4}*
k_2 /s^{-1}	*1.2 (±0.2) ×10^{-4}*	*1.3 (±0.2) ×10^{-4}*	*1.7 (±0.2) ×10^{-4}*	*2.5 (±0.2) ×10^{-4}*
P	*0.24 (±0.04)*	*0.26 (±0.04)*	*0.29 (±0.04)*	*0.34 (±0.02)*
R^2	*0.9963*	*0.9952*	*0.9970*	*0.9972*
		Simulated saliva		
C_{eq} / (□g mL^{-1})	*16.7 (±0.2)*	*30.2 (±0.3)*	*10.1 (±0.6)*	*14.6 (±0.6)*
$logt_1$ /s	*4468 (±363)*	*3948 (±529)*	*4906 (±300)*	*969 (±127)*
$logt_2$ / s	*13567 (±131)*	*13225 (±118)*	*13379 (±147)*	*11972 (±321)*
k_1 /s^{-1}	*2.9 (±0.4)×10^{-4}*	*2.0 (±0.3)×10^{-4}*	*2.7 (±0.3)×10^{-4}*	*8 (±2)×10^{-4}*
k_2 /s^{-1}	*3.3 (±0.3) ×10^{-4}*	*3.8 (±0.4) ×10^{-4}*	*3.3 (±0.4) ×10^{-4}*	*1.4 (±0.2) ×10^{-4}*
P	*0.34 (±0.03)*	*0.36 (±0.03)*	*0.43 (±0.04)*	*0.24 (±0.04)*
R^2	*0.9974*	*0.9978*	*0.9981*	*0.9951*

The values inside parenthesis are the standard deviations.

From the analysis of Figures 6 and 7 and C_{eq} summarized in the table 2, it can also be concluded that the amount of GP released is significantly higher in synthetic saliva than in water. The amount of GP released reaches a value between 14 and 36% of the encapsulated amount of GP. This may be justified by the ionic strength effect on these gels. Once both gels are ampholytic gels, an increase in the ionic strength may lead to a swelling effect which may stabilize both polymers [64, 65] and thus contributing for an enhancement of GP release. This is also followed by a significant increase in the EC50 for the first step

release (logt1), comparing with those observed for water system. A final remark concerns the contribution of both steps for the whole release process. In all systems, the first step mechanism contributes with ca. 30 % for the total release of GP, suggesting that the main release process is probably affected by some polymeric relaxation processes, further facilitating the mobility and release of the GP [66-68].

Biological Analysis

For the biological analysis, the results are showed in Figure 8.

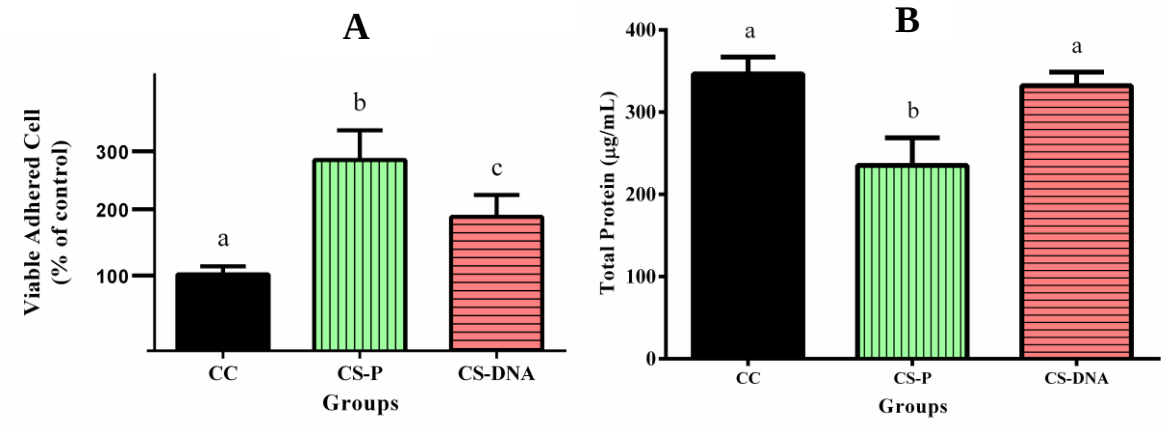

Figure 8*- Graphics reporting mean ± SD for in vitro tests: a) measurement of cell viability MTT assay; b) Total Protein production. Values that do not share the same superscript letters are significantly different from each other ($p<0.05$).*

The cell viability was obtained by MTT assay, and measurement of cell viability of experimental groups were compared to control group (100%) (Figure 8A). The CS-P and CS-DNA influenced positively in the cell culture and improved the number of viable cell. However CS-P experimental group exhibited statistical difference with control group ($p<0.0001$), which presented

the lower cell viability. This result is in accordance with previous studies, which was observed increase of viable cells in different linage cells when the Chi was used as biomaterial base [69-71]. The rates of cell viability exhibited by both groups make them suitable for biomedical use according to the International Organization for Standardization (ISO) and national standards for Biological Evaluation of Medical Devices, ISO 10993-5 [72].

Regarding to total protein (Figure 8B), there was no statistical difference between control group and CS-DNA (p>0.001), but the values from CS-P experimental group were lower than control group, with statistical difference (p=0.0002).

The results exhibited represents that these new biomaterials are acceptable in the biological environment and can provide evidence for the potential of biomimetic material for tissue engineering.

CONCLUSION

It can be concluded that the hydrogel complexation of Chitosan with DNA and Pectin is a viable alternative to drug delivery system of herbal medicine such as GP.

Acknowledgements

The authors are thankful to CAPES (Coordenação de Aperfeiçoamento de Pessoal de Nível Superior) for Sato TP sandwich-doctorate scholarship (Process 88881.189533/2018-01) in Coimbra University.

REFERENCES

1. Peppas NA. Hydrogels in medicine and pharmacy. Vol. 1, Fundamentals. Crc Press, 1986.

2. Ma S, Yu B, Pei X and Zhou F. Structural hydrogels. Polymer. 2016; 98: 516-35.

3. Gong JP. Friction and lubrication of hydrogels—its richness and complexity. Soft matter. 2006; 2: 544-52.

4. Can M, Ayyala RS and Sahiner N. Crosslinked poly(Lactose) microgels and nanogels for biomedical applications. Journal of colloid and interface science. 2019; 553: 805-12.

5. Qi X, Su T, Tong X, et al. Facile formation of salecan/agarose hydrogels with tunable structural properties for cell culture. Carbohydrate polymers. 2019; 224: 115208.

6. Costa D, Albuquerque T, Queiroz JA and Valente AJM. A co-delivery platform based on plasmid DNA peptide-surfactant complexes: formation, characterization and release behavior. Colloids and Surfaces B: Biointerfaces. 2019; 178: 430-8.

7. Croisfelt FM, Tundisi LL, Ataide JA, et al. Modified-release topical hydrogels: a ten-year review. Journal of Materials Science. 2019: 1-21.

8. Qin X, Zhang H, Wang Z and Jin Y. Magnetic chitosan/graphene oxide composite loaded with novel photosensitizer for enhanced photodynamic therapy. RSC Advances. 2018; 8: 10376-88.

9. Kyzas GZ and Bikiaris DN. Recent modifications of chitosan for adsorption applications: a critical and systematic review. Marine drugs. 2015; 13: 312-37.

10. Martins AF, Bueno PV, Almeida EA, Rodrigues FH, Rubira AF and Muniz EC. Characterization of N-trimethyl chitosan/alginate complexes and

curcumin release. International journal of biological macromolecules. 2013; 57: 174-84.

11. Hon D. Chitin and chitosan: medical applications. Polysaccharides in medicinal applications. 1996: 631-50.

12. Chien KB, Chung EJ and Shah RN. Investigation of soy protein hydrogels for biomedical applications: materials characterization, drug release, and biocompatibility. Journal of biomaterials applications. 2014; 28: 1085-96.

13. Berger J, Reist M, Mayer JM, Felt O and Gurny R. Structure and interactions in chitosan hydrogels formed by complexation or aggregation for biomedical applications. European Journal of Pharmaceutics and Biopharmaceutics. 2004; 57: 35-52.

14. Berger J, Reist M, Mayer JM, Felt O, Peppas N and Gurny R. Structure and interactions in covalently and ionically crosslinked chitosan hydrogels for biomedical applications. European journal of pharmaceutics and biopharmaceutics. 2004; 57: 19-34.

15. Aydınoğlu D and Ünal M. Evaluation of the influence of spirulina microalgae on the drug delivery characteristics of genipin cross-linked chitosan hydrogels. International Journal of Polymeric Materials and Polymeric Biomaterials. 2019; 68: 1020-33.

16. Reyna-Urrutia VA, Mata-Haro V, Cauich-Rodriguez JV, Herrera-Kao WA and Cervantes-Uc JM. Effect of two crosslinking methods on the physicochemical and biological properties of the collagen-chitosan scaffolds. European Polymer Journal. 2019; 117: 424-33.

17. Uzumcu AT, Guney O and Okay O. Nanocomposite DNA hydrogels with temperature sensitivity. Polymer. 2016; 100: 169-78.

18. Murakami Y and Maeda M. DNA-responsive hydrogels that can shrink or swell. Biomacromolecules. 2005; 6: 2927-9.

19. Ishizuka N, Hashimoto Y, Matsuo Y and Ijiro K. Highly expansive DNA hydrogel films prepared with photocrosslinkable poly (vinyl alcohol). Colloids and Surfaces A: Physicochemical and Engineering Aspects. 2006; 284: 440-3.

20. Costa D, Valente AJ, Miguel MG and Queiroz J. Gel network photodisruption: a new strategy for the codelivery of plasmid DNA and drugs. Langmuir : the ACS journal of surfaces and colloids. 2011; 27: 13780-9.

21. Li J, Fan C, Pei H, Shi J and Huang Q. Smart drug delivery nanocarriers with self-assembled DNA nanostructures. Advanced materials. 2013; 25: 4386-96.

22. Um SH, Lee JB, Park N, Kwon SY, Umbach CC and Luo D. Enzyme-catalysed assembly of DNA hydrogel. Nature materials. 2006; 5: 797.

23. Costa D, Valente AJM, Miguel MG and Queiroz J. Plasmid DNA hydrogels for biomedical applications. Advances in Colloid and Interface Science. 2014; 205: 257-64.

24. Costa D, Valente AJ and Queiroz J. Stimuli-responsive polyamine-DNA blend nanogels for co-delivery in cancer therapy. Colloids and surfaces B, Biointerfaces. 2015; 132: 194-201.

25. Costa D, Valente AJM, Queiroz JA and Sousa A. Finding the ideal polyethylenimine-plasmid DNA system for co-delivery of payloads in cancer therapy. Colloids and surfaces B, Biointerfaces. 2018; 170: 627-36.

26. Jorge AF, Dias RS, Pereira JC and Pais AACC. DNA Condensation by pH-Responsive Polycations. Biomacromolecules. 2010; 11: 2399-406.

27. Jorge AF, Morán MC, Vinardell MP, Pereira JC, Dias RS and Pais AA. Ternary complexes DNA–polyethylenimine–Fe (iii) with linear and branched polycations: implications on condensation, size, charge and in vitro biocompatibility. Soft Matter. 2013; 9: 10799-810.

28. Bravo-Anaya LM, Rinaudo M and Martínez FAS. Conformation and rheological properties of calf-thymus DNA in solution. Polymers. 2016; 8: 51.

29. Bravo-Anaya LM, Soltero JFA and Rinaudo M. DNA/chitosan electrostatic complex. International Journal of Biological Macromolecules. 2016; 88: 345-53.

30. Neufeld L and Bianco-Peled H. Pectin–chitosan physical hydrogels as potential drug delivery vehicles. International Journal of Biological Macromolecules. 2017; 101: 852-61.

31. Cesar Filho M, Bueno PV, Matsushita AF, et al. Synthesis, characterization and sorption studies of aromatic compounds by hydrogels of chitosan blended with β-cyclodextrin-and PVA-functionalized pectin. RSC Advances. 2018; 8: 14609-22.

32. Mohnen D. Pectin structure and biosynthesis. Current opinion in plant biology. 2008; 11: 266-77.

33. Thakur BR, Singh RK, Handa AK and Rao M. Chemistry and uses of pectin—a review. Critical Reviews in Food Science & Nutrition. 1997; 37: 47-73.

34. de Barros MP, Sousa JPB, Bastos JK and de Andrade SF. Effect of Brazilian green propolis on experimental gastric ulcers in rats. Journal of Ethnopharmacology. 2007; 110: 567-71.

35. Santos V, Pimenta F, Aguiar M, Do Carmo M, Naves M and Mesquita R. Oral candidiasis treatment with Brazilian ethanol propolis extract. Phytotherapy Research: An International Journal Devoted to Pharmacological and Toxicological Evaluation of Natural Product Derivatives. 2005; 19: 652-4.

36. Nakajima Y, Shimazawa M, Mishima S and Hara H. Water extract of propolis and its main constituents, caffeoylquinic acid derivatives, exert neuroprotective effects via antioxidant actions. Life Sciences. 2007; 80: 370-7.

37. Guimarães NS, Mello JC, Paiva JS, et al. Baccharis dracunculifolia, the main source of green propolis, exhibits potent antioxidant activity and prevents

oxidative mitochondrial damage. Food and Chemical Toxicology. 2012; 50: 1091-7.

38. Bankova VS, de Castro SL and Marcucci MC. Propolis: recent advances in chemistry and plant origin. Apidologie. 2000; 31: 3-15.

39. Swartz ML, Phillips RW and Daoud El Tannir M. Tarnish of certain dental alloys. Journal of dental Research. 1958; 37: 837-47.

40. Fusayama T, Katayori T and Nomoto S. Corrosion of gold and amalgam placed in contact with each other. Journal of Dental Research. 1963; 42: 1183-97.

41. Nomura D, Saito M, Takahashi Y, Takahashi Y, Takakura Y and Nishikawa M. Development of Orally-deliverable DNA Hydrogel by Microemulsification and Chitosan Coating. International journal of pharmaceutics. 2018.

42. Grande R and Carvalho AJ. Compatible ternary blends of chitosan/poly (vinyl alcohol)/poly (lactic acid) produced by oil-in-water emulsion processing. Biomacromolecules. 2011; 12: 907-14.

43. Papancea A, Valente AJ, Patachia S, Miguel MG and Lindman B. PVA−DNA cryogel membranes: Characterization, swelling, and transport studies. Langmuir : the ACS journal of surfaces and colloids. 2008; 24: 273-9.

44. Prado RFd, de Oliveira FS, Nascimento RD, de Vasconcellos LMR, Carvalho YR and Cairo CAA. Osteoblast response to porous titanium and biomimetic surface: In vitro analysis. Materials Science and Engineering: C. 2015; 52: 194-203.

45. Fernandes Queiroz M, Melo KR, Sabry DA, Sassaki GL and Rocha HA. Does the use of chitosan contribute to oxalate kidney stone formation? Mar Drugs. 2014; 13: 141-58.

46. Souza NLGD, Salles TF, Brandão HM, Edwards HGM and Oliveira LFCd. Synthesis, Vibrational Spectroscopic and Thermal Properties of

Oxocarbon Cross Linked Chitosan. Journal of the Brazilian Chemical Society. 2015; 26: 1247-56.

47. Krishnaveni B and Ragunathan R. Extraction and Characterization of Chitin and Chitosan from F. solani CBNR BKRR, Synthesis of their Bionanocomposites and Study of their Productive Application. Journal of Pharmaceutical Sciences and Research. 2015; 7: 197.

48. Gnanasambandam R and Proctor A. Determination of pectin degree of esterification by diffuse reflectance Fourier transform infrared spectroscopy. Food Chemistry. 2000; 68: 327-32.

49. Silverstein RM and Bassler GC. Spectrometric identification of organic compounds. Journal of Chemical Education. 1962; 39: 546.

50. Lindqvist M and Gräslund A. An FTIR and CD study of the structural effects of G-tract length and sequence context on DNA conformation in solution. Journal of molecular biology. 2001; 314: 423-32.

51. Ede SR, Ramadoss A, Anantharaj S, Nithiyanantham U and Kundu S. Enhanced catalytic and supercapacitor activities of DNA encapsulated β-MnO 2 nanomaterials. Physical Chemistry Chemical Physics. 2014; 16: 21846-59.

52. Froehlich E, Mandeville J, Weinert C, Kreplak L and Tajmir-Riahi H. Bundling and aggregation of DNA by cationic dendrimers. Biomacromolecules. 2010; 12: 511-7.

53. Rachini A, Le Troedec M, Peyratout C and Smith A. Comparison of the thermal degradation of natural, alkali-treated and silane-treated hemp fibers under air and an inert atmosphere. Journal of applied polymer science. 2009; 112: 226-34.

54. Liu Y, Sun Y, Ding G, et al. Synthesis, Characterization, and Application of Microbe-Triggered Controlled-Release Kasugamycin–Pectin Conjugate. Journal of agricultural and food chemistry. 2015; 63: 4263-8.

55. Corazzari I, Nisticò R, Turci F, et al. Advanced physico-chemical characterization of chitosan by means of TGA coupled on-line with FTIR and GCMS: Thermal degradation and water adsorption capacity. Polymer Degradation and Stability. 2015; 112: 1-9.

56. Safaee MM, Gravely M, Lamothe A, McSweeney M and Roxbury D. Enhancing the Thermal Stability of Carbon Nanomaterials with DNA. Scientific Reports. 2019; 9: 11926.

57. Stealey S, Guo X, Ren L, et al. Stability improvement and characterization of bioprinted pectin-based scaffold. Journal of Applied Biomaterials & Functional Materials. 2019; 17: 2280800018807108.

58. Cazorla-Luna R, Notario-Pérez F, Martín-Illana A, et al. Chitosan-Based Mucoadhesive Vaginal Tablets for Controlled Release of the Anti-HIV Drug Tenofovir. Pharmaceutics. 2019; 11: 20.

59. Macha IJ, Ben-Nissan B, Vilchevskaya EN, et al. Drug Delivery From Polymer-Based Nanopharmaceuticals—An Experimental Study Complemented by Simulations of Selected Diffusion Processes. Frontiers in Bioengineering and Biotechnology. 2019; 7.

60. Peppas NA and Sahlin JJ. A simple equation for the description of solute release. III. Coupling of diffusion and relaxation. International Journal of Pharmaceutics. 1989; 57: 169-72.

61. Issa MG, Pessole L, Takahashi AI, Andréo Filho N and Ferraz HG. Physicochemical and dissolution profile characterization of pellets containing different binders obtained by the extrusion-spheronization process. Brazilian Journal of Pharmaceutical Sciences. 2012; 48: 379-88.

62. Costa D, Valente AJM, Miguel MG and Queiroz J. Gel Network Photodisruption: A New Strategy for the Codelivery of Plasmid DNA and Drugs. Langmuir : the ACS journal of surfaces and colloids. 2011; 27: 13780-9.

63. Liu L and Hu S. Optimizing the Synthesis of Core/shell Structure Au@Cu2S Nanocrystals as Contrast-enhanced for Bioimaging Detection. 2018; 8: 8866.

64. Baker JP, Stephens DR, Blanch HW and Prausnitz JM. Swelling equilibria for acrylamide-based polyampholyte hydrogels. Macromolecules. 1992; 25: 1955-8.

65. Valente AJM, Cruz SMA, Murtinho DMB, Miguel MG and Muniz EC. DNA–poly(vinyl alcohol) gel matrices: Release properties are strongly dependent on electrolytes and cationic surfactants. Colloids and Surfaces B: Biointerfaces. 2013; 101: 111-7.

66. Siepmann J, Podual K, Sriwongjanya M, Peppas NA and Bodmeier R. A new model describing the swelling and drug release kinetics from hydroxypropyl methylcellulose tablets. Journal of pharmaceutical sciences. 1999; 88: 65-72.

67. Faisant N, Siepmann J and Benoit JP. PLGA-based microparticles: elucidation of mechanisms and a new, simple mathematical model quantifying drug release. European journal of pharmaceutical sciences : official journal of the European Federation for Pharmaceutical Sciences. 2002; 15: 355-66.

68. Polishchuk AY and Zaikov GE. Multicomponent Transport in Polymer Systems for Controlled Release. Gordon and Breach, 1997.

69. Dinescu S, Ionita M, Ignat S-R, Costache M and Hermenean A. Graphene Oxide Enhances Chitosan-Based 3D Scaffold Properties for Bone Tissue Engineering. International Journal of Molecular Sciences. 2019; 20: 5077.

70. Li Y, Qiao Z, Yu F, Hu H, Huang Y and Xiang Q. Transforming Growth Factor-beta3/Chitosan Sponge (TGF-beta3/CS) Facilitates Osteogenic Differentiation of Human Periodontal Ligament Stem Cells. 2019; 20.

71. Singh YP, Dasgupta S and Bhaskar R. Preparation, characterization and bioactivities of nano anhydrous calcium phosphate added gelatin–chitosan

scaffolds for bone tissue engineering. Journal of Biomaterials Science, Polymer Edition. 2019; 30: 1756-78.

72. Normalizacyjny PPK. Biological Evaluation of Medical Devices - Part 5: Tests for in Vitro Cytotoxicity (ISO 10993-5:2009). Polski Komitet Normalizacyjny, 2009.

3 CONSIDERAÇÕES GERAIS

Sob os aspectos atuais do desenvolvimento de biomateriais, a proposição do presente estudo delineou a produção de duas diferentes matrizes à base de um biopolímero já utilizado para diferentes aplicações biomédicas, a quitosana. (Berger et al., 2005; Cheung et al., 2015).

A primeira matriz desenvolvida, um arcabouço de fibras ultrafinas eletrofiadas com e sem inclusão de cristais de nanohidroxiapatita se comportou como um material biomimético, promovendo a diferenciação celular. E especificamente em relação à diferenciação osteoblástica, a associação de hidroxiapatita e polímeros apresenta resultados positivos para o metabolismo celular (Wutticharoenmongkol et al., 2007). Assim, neste estudo, ChHa proporcionou maiores médias de atividade de fosfatase alcalina, sendo que este é um indicador precoce da diferenciação dos osteoblastos e sua expressão é considerada um parâmetro funcional in vitro, refletindo o progresso da diferenciação celular (Hoemann et al., 2009).

A segunda matriz desenvolvida, um hidrogel, foi subdividida em um hidrogel de quitosana coacervado com DNA de salmão e um hidrogel de quitosana coacervado com Pectina. Ambas apresentaram potencial para liberação controlada de fármacos. Pode-se observar que, em todos os casos estudados, a cinética de liberação segue um mecanismo de duas etapas que ocorrem concomitantemente, já que nenhum platô é observado. As duas etapas contribuem para todo o processo de liberação. Em todos os sistemas, o mecanismo da primeira etapa contribui com 30% para a liberação total do GP, sugerindo que o processo principal de liberação provavelmente é afetado por alguns processos de relaxamento polimérico, facilitando ainda mais a mobilidade e a liberação do GP (Faisant et al., 2002; Polishchuk, Zaikov, 1997;

Siepmann et al., 1999).

Assim sendo, considerando as limitações metodológicas empregadas, foi possível desenvolver e caracterizar dois materiais com potenciais de atuação complementar.

Sugere-se com isso, que as possíveis aplicações de ambos materiais podem se delinear da seguinte maneira: clinicamente, a matriz de fibras poderá atuar como uma membrana de regeneração óssea guiada, para posterior instalação de implante osseointegrado, e o hidrogel poderá ser utilizado como um mecanismo de terapia profilática, utilizado entre os componentes das próteses sobre implantes, evitando a proliferação microbiana ou mesmo na superfície de implantes no tratamento da periimplantite.

REFERÊNCIAS*

Ahmed FE, Lalia BS, Hashaikeh R. A review on electrospinning for membrane fabrication: challenges and applications. Desalination. 2015;356:15-30. doi: 10.1016/j.desal.2014.09.033

AlKahtani RN. The implications and applications of nanotechnology in dentistry: A review. Saudi Dent J. 2018;30(2):107-16. doi: 10.1016/j.sdentj.2018.01.002

Atala A. Tissue engineering and regenerative medicine: concepts for clinical application. Rejuvenation Res. 2004;7(1):15-31. doi: 10.1089/154916804323105053

Aykut-Yetkiner A, Attin T, Wiegand A. Prevention of dentine erosion by brushing with anti-erosive toothpastes. J Dent. 2014;42(7):856-61. doi: 10.1016/j.jdent.2014.03.011

Bankova VS, de Castro SL, Marcucci MC. Propolis: recent advances in chemistry and plant origin. Apidologie. 2000;31(1):3-15. doi: 10.1051/apido:2000102

Barbosa MC, Messmer NR, Brazil TR, Marciano FR, Lobo AO. The effect of ultrasonic irradiation on the crystallinity of nano-hydroxyapatite produced via the wet chemical method. Mater Sci Eng C Mater Biol Appl. 2013;33(5):2620-5. doi: 10.1016/j.msec.2013.02.027

Berger J, Reist M, Chenite A, Felt-Baeyens O, Mayer J, Gurny R. Pseudo-thermosetting chitosan hydrogels for biomedical application. Int. J Pharm. 2005;288(2):197-206. doi: 10.1016/j.ijpharm.2004.07.037

Bonassar LJ, Vacanti CA. Tissue engineering: the first decade and beyond. J Cell Biochem Suppl. 1998;30-31:297-303. doi: 10.1002/(SICI)1097-4644(1998)72:30/31+<297::AID-JCB36>3.0.CO;2-6

Boyapalle S, Xu W, Raulji P, Mohapatra S, Mohapatra SS. A Multiple siRNA-Based Anti-HIV/SHIV Microbicide Shows Protection in Both In Vitro and In Vivo Models. PLoS One. 2015;10(9):e0135288. doi: 10.1371/journal.pone.0135288

---

* Baseado em: International Committee of Medical Journal Editors Uniform Requirements for Manuscripts Submitted to Biomedical journals: Sample References [Internet]. Bethesda: US NLM; c2003 [cited 2019 Jan 2019]. U.S. National Library of Medicine; [about 6 p.]. Available from: http://www.nlm.nih.gov/bsd/uniform_requirements.html

Bravo-Anaya LM, Rinaudo M, Martínez FAS. Conformation and rheological properties of calf-thymus DNA in solution. Polymers. 2016a;8(2):51. doi: 10.3390/polym8020051

Bravo-Anaya LM, Soltero JFA, Rinaudo M. DNA/chitosan electrostatic complex. Int. J Biol Macromol. 2016b;88:345-53. doi: 10.1016/j.ijbiomac.2016.03.035

Cesar Filho M, Bueno PV, Matsushita AF, Rubira AF, Muniz EC, Durães L, et al. Synthesis, characterization and sorption studies of aromatic compounds by hydrogels of chitosan blended with β-cyclodextrin-and PVA-functionalized pectin. RSC Advances. 2018;8(26):14609-22. doi:

Charernsriwilaiwat N, Rojanarata T, Ngawhirunpat T, Sukma M, Opanasopit P. Electrospun chitosan-based nanofiber mats loaded with Garcinia mangostana extracts. Int. J. Pharm. 2013;452(1–2):333-43. doi: 10.1016/j.ijpharm.2013.05.012

Chen J, Liu C, Shan W, Xiao Z, Guo H, Huang Y. Enhanced stability of oral insulin in targeted peptide ligand trimethyl chitosan nanoparticles against trypsin. J Microencapsul. 2015:1-10. doi: 10.3109/02652048.2015.1065920

Chen Z, Mo X, Qing F. Electrospinning of collagen–chitosan complex. Mater Lett. 2007;61(16):3490-4. doi: 10.1016/j.matlet.2006.11.104

Chen ZG, Wang PW, Wei B, Mo XM, Cui FZ. Electrospun collagen–chitosan nanofiber: A biomimetic extracellular matrix for endothelial cell and smooth muscle cell. Acta Biomater. 2010;6(2):372-82. doi: doi: 10.1016/j.actbio.2009.07.024

Cheung RCF, Ng TB, Wong JH, Chan WY. Chitosan: an update on potential biomedical and pharmaceutical applications. Mar Drugs. 2015;13(8):5156-86. doi: 10.3390/md13085156

Chung BG, Kang L, Khademhosseini A. Micro- and nanoscale technologies for tissue engineering and drug discovery applications. Exp Op Drug Disc. 2007;2(12):1653-68. doi: 10.1517/17460441.2.12.1653

Costa D, Albuquerque T, Queiroz JA, Valente AJM. A co-delivery platform based on plasmid DNA peptide-surfactant complexes: formation, characterization and release behavior. Colloids Surf B Biointerfaces. 2019;178:430-8. doi: 10.1016/j.colsurfb.2019.03.029

Costa D, Valente AJ, Miguel MG, Queiroz J. Gel network photodisruption: a new strategy for the codelivery of plasmid DNA and drugs. Langmuir. 2011;27(22):13780-9. doi: 10.1021/la2026285

Costa D, Valente AJ, Queiroz J. Stimuli-responsive polyamine-DNA blend nanogels for co-delivery in cancer therapy. Colloids Surf B Biointerfaces. 2015;132:194-201. doi: 10.1016/j.colsurfb.2015.04.064

Costa D, Valente AJM, Miguel MG, Queiroz J. Plasmid DNA hydrogels for biomedical applications. Adv Colloid Interface Sci. 2014;205:257-64. doi: https://doi.org/10.1016/j.cis.2013.08.002

Costa D, Valente AJM, Queiroz JA, Sousa A. Finding the ideal polyethylenimine-plasmid DNA system for co-delivery of payloads in cancer therapy. Colloids Surf B Biointerfaces. 2018;170:627-36. doi: 10.1016/j.colsurfb.2018.06.063

de Barros MP, Sousa JPB, Bastos JK, de Andrade SF. Effect of Brazilian green propolis on experimental gastric ulcers in rats. J Ethnopharmacol. 2007;110(3):567-71. doi: 10.1016/j.jep.2006.10.022

Faisant N, Siepmann J, Benoit JP. PLGA-based microparticles: elucidation of mechanisms and a new, simple mathematical model quantifying drug release. Eur J Pharm Sci. 2002;15(4):355-66. doi: 10.1016/S0928-0987(02)00023-4

Feng L, Li S, Li H, Zhai J, Song Y, Jiang L, et al. Super-Hydrophobic Surface of Aligned Polyacrylonitrile Nanofibers. Angew Chem Int Ed. 2002;41(7):1221-3. doi: 10.1002/1521-3773(20020402)41:7<1221::aid-anie1221>3.0.co;2-g

Foster LJR, Ho S, Hook J, Basuki M, Marçal H. Chitosan as a Biomaterial: Influence of Degree of Deacetylation on Its Physiochemical, Material and Biological Properties. PLoS One. 2015;10(8):e0135153. doi: 10.1371/journal.pone.0135153

Frenot A, Chronakis IS. Polymer nanofibers assembled by electrospinning. Curr Opin Colloid Interface Sci. 2003;8(1):64-75. doi: 10.1016/S1359-0294(03)00004-9

Geng X, Kwon O-H, Jang J. Electrospinning of chitosan dissolved in concentrated acetic acid solution. Biomaterials. 2005;26(27):5427-32. doi: 10.1016/j.biomaterials.2005.01.066

Gong JP. Friction and lubrication of hydrogels—its richness and complexity. Soft matter. 2006;2(7):544-52. doi: 10.1039/b603209p

Gopalan Nair K, Dufresne A. Crab Shell Chitin Whisker Reinforced Natural Rubber Nanocomposites. 1. Processing and Swelling Behavior. Biomacromolecules. 2003;4(3):657-65. doi: 10.1021/bm020127b

Guimarães NS, Mello JC, Paiva JS, Bueno PC, Berretta AA, Torquato RJ, et al. Baccharis dracunculifolia, the main source of green propolis, exhibits potent antioxidant activity and prevents oxidative mitochondrial damage. Food Chem Toxicol. 2012;50(3-4):1091-7. doi: 10.1016/j.fct.2011.11.014

Hadipour-Goudarzi E, Montazer M, Latifi M, Aghaji AAG. Electrospinning of chitosan/sericin/PVA nanofibers incorporated with in situ synthesis of nano silver. Carbohydr Polym. 2014;113:231-9. doi: 10.1016/j.carbpol.2014.06.082

Hiraoka S. What Do We Learn from the Molecular Self-Assembly Process? Chem Rec. 2015;15(6): 1144-1147. doi: 10.1002/tcr.201510005

Hoemann CD, El-Gabalawy H, McKee MD. In vitro osteogenesis assays: Influence of the primary cell source on alkaline phosphatase activity and mineralization. Pathol Biol. 2009;57(4):318-23. doi: 10.1016/j.patbio.2008.06.004

Homayoni H, Ravandi SAH, Valizadeh M. Electrospinning of chitosan nanofibers: processing optimization. Carbohydr Polym. 2009;77(3):656-61. doi: 10.1016/j.carbpol.2009.02.008

Honarkar H, Barikani M. Applications of biopolymers I: chitosan. Monatsh Chem. 2009;140(12):1403-20. doi: 10.1007/s00706-009-0197-4

Huang Z-M, Zhang YZ, Kotaki M, Ramakrishna S. A review on polymer nanofibers by electrospinning and their applications in nanocomposites. Compos Sci Technol. 2003;63(15):2223-53. doi: 10.1016/S0266-3538(03)00178-7

Ifuku S. Chitin and Chitosan Nanofibers: Preparation and Chemical Modifications. Molecules. 2014;19(11):18367. doi: 10.3390/molecules191118367

Ishizuka N, Hashimoto Y, Matsuo Y, Ijiro K. Highly expansive DNA hydrogel films prepared with photocrosslinkable poly (vinyl alcohol). Colloid Surf A Physicochem Eng Asp. 2006;284:440-3. doi: 10.1016/j.colsurfa.2005.11.027

Jorge AF, Dias RS, Pereira JC, Pais AACC. DNA Condensation by pH-Responsive Polycations. Biomacromolecules. 2010;11(9):2399-406. doi: 10.1021/bm100565r

Jorge AF, Morán MC, Vinardell MP, Pereira JC, Dias RS, Pais AA. Ternary complexes DNA–polyethylenimine–Fe (iii) with linear and branched polycations: implications on condensation, size, charge and in vitro biocompatibility. Soft Matter. 2013;9(45):10799-810. doi:

Karpova S, Ol'khov A, Iordanskii A, Lomakin S, Shilkina N, Popov A, et al. Nonwoven blend composites based on poly (3-hydroxybutyrate)–chitosan ultrathin fibers prepared via electrospinning. Polym Sci Ser A. 2016;58(1):76-86. doi: 10.1134/S0965545X16010041

Kingsley DJ, Shivendu R, Nandita D, Proud S. Nanotechnology for tissue engineering: Need, techniques and applications. J Pharm Res. 2013;7(2):200-4. doi: 10.1016/j.jopr.2013.02.021

Kong L, Gao Y, Lu G, Gong Y, Zhao N, Zhang X. A study on the bioactivity of chitosan/nano-hydroxyapatite composite scaffolds for bone tissue engineering. Eur Polym J. 2006;42(12):3171-9. doi: 10.1016/j.eurpolymj.2006.08.009

Kumar PS, Jayaraman S, Singh G. Polymer and Composite Nanofiber: Electrospinning Parameters and Rheology Properties. Rheology and Processing of Polymer Nanocomposites. 2016. p. 329-54.

Li J, Fan C, Pei H, Shi J, Huang Q. Smart drug delivery nanocarriers with self-assembled DNA nanostructures. Adv Mater 2013;25(32):4386-96. doi: 10.1002/adma.201300875

Liu Y, Liu Y, Liao N, Cui F, Park M, Kim H-Y. Fabrication and durable antibacterial properties of electrospun chitosan nanofibers with silver nanoparticles. Int. J Biol Macromol. 2015;79:638-43. doi: 10.1016/j.ijbiomac.2015.05.058

Lyons J, Li C, Ko F. Melt-electrospinning part I: processing parameters and geometric properties. Polymer. 2004;45(22):7597-603. doi: 10.1016/j.polymer.2004.08.071

Ma S, Chen Z, Qiao F, Sun Y, Yang X, Deng X, et al. Guided bone regeneration with tripolyphosphate cross-linked asymmetric chitosan membrane. J Dent. 2014;42(12):1603-12. doi: 10.1016/j.jdent.2014.08.015

Ma S, Yu B, Pei X, Zhou F. Structural hydrogels. Polymer. 2016;98:516-35. doi: 10.1016/j.polymer.2016.06.053

Martin CR. Membrane-Based Synthesis of Nanomaterials. Chem Mater. 1996;8(8):1739-46. doi: 10.1021/cm960166s

Mehrasa M, Asadollahi MA, Ghaedi K, Salehi H, Arpanaei A. Electrospun aligned PLGA and PLGA/gelatin nanofibers embedded with silica nanoparticles for tissue engineering. Int. J Biol Macromol. 2015;79:687-95. doi: 10.1016/j.ijbiomac.2015.05.050

Mohnen D. Pectin structure and biosynthesis. Curr Opin Plant Biol. 2008;11(3):266-77. doi: 10.1016/j.pbi.2008.03.006

Murakami Y, Maeda M. DNA-responsive hydrogels that can shrink or swell. Biomacromolecules. 2005;6(6):2927-9. doi: 10.1021/bm0504330

Nakajima Y, Shimazawa M, Mishima S, Hara H. Water extract of propolis and its main constituents, caffeoylquinic acid derivatives, exert neuroprotective effects via antioxidant actions. Life Sci. 2007;80(4):370-7. doi: 10.1016/j.lfs.2006.09.017

Neufeld L, Bianco-Peled H. Pectin–chitosan physical hydrogels as potential drug delivery vehicles. Int. J Biol Macromol. 2017;101:852-61. doi: 10.1016/j.ijbiomac.2017.03.167

Nga NK, Giang LT, Huy TQ, Viet PH, Migliaresi C. Surfactant-assisted size control of hydroxyapatite nanorods for bone tissue engineering. Colloids Surf B Biointerfaces. 2014;116:666-73. doi: 10.1016/j.colsurfb.2013.11.001

Ngwuluka NC, Ochekpe NA, Aruoma OI. Functions of Bioactive and Intelligent Natural Polymers in the Optimization of Drug Delivery. Industrial Applications for Intelligent Polymers and Coatings: Springer. 2016. p. 165-84.

Ohkawa K, Cha D, Kim H, Nishida A, Yamamoto H. Electrospinning of chitosan. Macromol Rapid Commun. 2004;25(18):1600-5. doi: 10.1002/marc.200400253

Ondarçuhu T, Joachim C. Drawing a single nanofibre over hundreds of microns. Europhys Lett. 1998;42(2):215. doi: 10.1209/epl/i1998-00233-9

Peppas NA. Hydrogels in medicine and pharmacy. Boca Raton: CRC; 1986.

Polishchuk AY, Zaikov GE. Multicomponent Transport in Polymer Systems for Controlled Release. Moscow. Gordon and Breach Sciences Publichers; 1997.

Qasim SB, Najeeb S, Delaine-Smith RM, Rawlinson A, Ur Rehman I. Potential of electrospun chitosan fibers as a surface layer in functionally graded GTR membrane for periodontal regeneration. Dent Mater. 2017;33(1):71-83. doi: 10.1016/j.dental.2016.10.003

Reneker DH, Chun I. Nanometre diameter fibres of polymer, produced by electrospinning. Nanotechnology. 1996;7(3):216. doi: 10.1088/0957-4484/7/3/009/meta

Sandreschi S, Piras AM, Batoni G, Chiellini F. Perspectives on polymeric nanostructures for the therapeutic application of antimicrobial peptides. Nanomedicine. 2016;11(13):1729-44. doi: 10.2217/nnm-2016-0057

Santos V, Pimenta F, Aguiar M, Do Carmo M, Naves M, Mesquita R. Oral candidiasis treatment with Brazilian ethanol propolis extract. Phytother Res. 2005;19(7):652-4. doi: 10.1002/ptr.1715

Sell SA, Wolfe PS, Garg K, McCool JM, Rodriguez IA, Bowlin GL. The use of natural polymers in tissue engineering: a focus on electrospun extracellular matrix analogues. Polymers. 2010;2(4):522-53. doi:

Shanmuga Sundar S, Sangeetha D. Investigation on sulphonated PEEK beads for drug delivery, bioactivity and tissue engineering applications. J Mater Sci. 2012;47(6):2736-42. doi: 10.1007/s10853-011-6100-9

Siepmann J, Podual K, Sriwongjanya M, Peppas NA, Bodmeier R. A new model describing the swelling and drug release kinetics from hydroxypropyl methylcellulose tablets. J Pharm Sci. 1999;88(1):65-72. doi: 10.1021/js9802291

Soares RM, Siqueira NM, Prabhakaram MP, Ramakrishna S. Electrospinning and electrospray of bio-based and natural polymers for biomaterials development. Mater Sci Eng C Mater Biol Appl. 2018;92:969-82. doi: 10.1016/j.msec.2018.08.004

Sun Y, Scarabelli L, Kotov N, Tebbe M, Lin XM, Brullot W, et al. Field-assisted self-assembly process: general discussion. Faraday Discuss. 2015;181:463-79. doi: 10.1039/C5FD90041G

Thakur BR, Singh RK, Handa AK, Rao M. Chemistry and uses of pectin—a review. Crit Rev Food Sci Nutr. 1997;37(1):47-73. doi: 10.1080/10408399709527767

Titorencu I, Georgiana Albu M, Nemecz M, V Jinga V. Natural Polymer-Cell Bioconstructs for Bone Tissue Engineering. Curr Stem Cell Res T. 2017;12(2):165-74. doi: 10.2174/1574888X10666151102105659

Um SH, Lee JB, Park N, Kwon SY, Umbach CC, Luo D. Enzyme-catalysed assembly of DNA hydrogel. Natur Mater. 2006;5(10):797. doi: 10.1038/nmat1741

Uzumcu AT, Guney O, Okay O. Nanocomposite DNA hydrogels with temperature sensitivity. Polymer. 2016;100:169-78. doi: 10.1016/j.polymer.2016.08.041

Wu Y, Feng S, Zan X, Lin Y, Wang Q. Aligned Electroactive TMV Nanofibers as Enabling Scaffold for Neural Tissue Engineering. Biomacromolecules. 2015. doi: 10.1021/acs.biomac.5b00884

Wutticharoenmongkol P, Pavasant P, Supaphol P. Osteoblastic Phenotype Expression of MC3T3-E1 Cultured on Electrospun Polycaprolactone Fiber Mats Filled with Hydroxyapatite Nanoparticles. Biomacromolecules. 2007;8(8):2602-10. doi: 10.1021/bm700451p

Xing X, Wang Y, Li B. Nanofibers drawing and nanodevices assembly in poly (trimethylene terephthalate). Optic Express. 2008;16(14):10815-22. doi: 10.1364/OE.16.010815

Zhang M, Guo J, Yu Y, Wu Y, Yun H, Jishkariani D, et al. 3D Nanofabrication via Chemo-Mechanical Transformation of Nanocrystal/Bulk Heterostructures. Adv Mater. 2018;30(22):1800233. doi: 10.1002/adma.201800233

Zhou H, Lee J. Nanoscale hydroxyapatite particles for bone tissue engineering. Acta Biomater. 2011;7(7):2769-81. doi: 10.1016/j.actbio.2011.03.019

ANEXO A – Comprovante de artigo enviado para publicação

Australian Dental Journal

Home

Author

Review

Submission Confirmation

Print

Thank you for your submission

Submitted to
Australian Dental Journal

Manuscript ID
ADJ-04-18-0198

Title
Potential of nanohydroxyapatite loading on electrospun chitosan fibers: biological and morphological studies

Authors
Sato, Tabata
Rodrigues, Bruno
Mello, Daphne
Machado, João Paulo
Bottino, Marco Cicero
Vasconcellos, Luana
Lobo, Anderson
Borges, Alexandre Luiz

Date Submitted
16-Apr-2018

Author Dashboard

ANEXO B – Certificado do Comitê de Ética em Pesquisa

UNIVERSIDADE ESTADUAL PAULISTA
"JÚLIO DE MESQUITA FILHO"
Campus de São José dos Campos
Instituto de Ciência e Tecnologia

CERTIFICADO
CEUA – Comissão de Ética no Uso de Animais

CERTIFICAMOS, que o protocolo registrado sob o nº 01/2017, intitulado:- "**Eletrofiação via solução de fibras ultrafinas de quitosana com nanohidroxiapatita: caracterização física e biológica** " sob a responsabilidade de **LUANA MAROTTA REIS DE VASCONCELLOS ,** tendo como colaboradora :- Tábata do Prado Sato, e que envolve a utilização de animais pertencentes ao filo Chordata subfilo Vertebrata (exceto humanos), para fins de pesquisa científica, encontra-se de acordo com os preceitos da Lei nº 11.794, de 8 de outubro de 2008, do Decreto nº 6.899 de 15 de julho de 2009 e com as Normas editadas pelo Conselho Nacional de Controle de Experimentação Animal (CONCEA), e foi **APROVADO** pela **COMISSÃO DE ÉTICA NO USO DE ANIMAIS** (CEUA – ICT – CAMPUS DE SÃO JOSÉ DOS CAMPOS-UNESP), em reunião de 07/04/2017.

Finalidade	( ) Ensino (X) Pesquisa Científica
Vigência da Autorirzação	07/04/2017 a 20/12/2018
Espécie/linhagem/raça	Rato/heterogênico Wistar
Nº de Animais	20
Peso/Idade	400 grs / 90 dias
Sexo	macho
Origem	Biotério Central – Campus de Botucatu-UNESP

São José dos Campos, 07 de abril de 2017

Profa.Dra. **PAULA CAROLINA KOMORI DE CARVALHO**
Coordenadora

Av. Eng. Francisco José Longo, 777 – Jd. São Dimas
CEP 12201-970 – F. (12) 3947-9028 / 9076
Fax (12) 3947-9010 / guedes@fosjc.unesp.br/komori@fosjc.unesp.br